Coordination Chemistry Reviews 255 (2011) 757–773

Contents lists available at ScienceDirect

Coordination Chemistry Reviews

journal homepage: www.elsevier.com/locate/ccr

Review

Electron transfer in blue copper proteins

Ole Farver[a,*], Israel Pecht[b]

[a] Institute of Analytical Chemistry, University of Copenhagen, 2 Universitetsparken, 2100 Copenhagen, Denmark
[b] Department of Immunology, The Weizmann Institute of Science, 76100 Rehovot, Israel

Contents

1. Introduction 758
2. ET theory and pulse radiolysis techniques 758
   2.1. Theory 758
   2.2. Pulse radiolysis 758
3. Single copper proteins 759
   3.1. Azurins 759
   3.2. Stellacyanin 762
4. Multi-copper enzymes 762
   4.1. Copper containing nitrite reductases (CuNiRs) 763
   4.2. Multi-copper oxidases 764
      4.2.1. Intramolecular ET in ascorbate oxidase and ceruloplasmin 764
      4.2.2. Intramolecular ET processes in laccases 768
      4.2.3. Formation of O_2 intermediates during MCO catalysis 770
5. Conclusions 772
   Acknowledgements 772
   References 772

ARTICLE INFO

Article history:
Received 25 June 2010
Accepted 10 August 2010
Available online 18 August 2010

Keywords:
Activation parameters
Ascorbate oxidase
Azurin
Ceruloplasmin
Driving force
Electron transfer
Intramolecular electron transfer
Laccase
Marcus equation
Nitrite reductase
Oxidase
Pathway
Pulse radiolysis
Radical
Reorganization
Stellacyanin
Time-resolved absorption
Type1 copper
Type2 copper
Type3 copper

ABSTRACT

This article reviews use of the pulse radiolysis technique in studies of intramolecular electron transfer processes in single- and multi-copper blue proteins. Kinetic parameters are analyzed in order to correlate rates and activation parameters with the available structural information. Reaction mechanisms are presented as well as current theoretical treatments based on the semi-classical Marcus theory.

Abbreviations: AO, ascorbate oxidase; AcNiR, *Achromobacter cycloclastes* nitrite reductase; AxNiR, *Alcaligenes xylosoxidans* nitrite reductase; CuNiRs, copper containing nitrite reductases; ET, electron transfer; hCp, human ceruloplasmin; LRET, long range ET; 1-MNA, 1-methyl-nicotinamide; MCO, multi-copper oxidase; PR, pulse radiolysis; TNC, three copper nuclear cluster; 3-D, three-dimensional; T1, type 1; T2, type 2; T3, type 3; WT, wild type.

* Corresponding author. Tel.: +45 4587 0065.
E-mail address: of@farma.ku.dk (O. Farver).

0010-8545/$ – see front matter © 2010 Elsevier B.V. All rights reserved.
doi:10.1016/j.ccr.2010.08.005

1. Introduction

The biological functions of copper ions are mainly electron mediation and catalysis of redox reactions. Copper proteins are involved in a wide range of electron transfer (ET) processes, predominantly in biological energy conversion cycles [1] but also in diverse biochemical transformations such as in metabolism. Our understanding of the electronic and functional properties of copper proteins has advanced dramatically particularly due to the high-resolution three-dimensional (3-D) structures of these proteins [2] now available. Structural information has allowed the analysis of rates and activation parameters of ET processes in relation to their reaction mechanisms and current theoretical treatments.

A major group of copper containing ET proteins, the so-called "blue" proteins, is widespread in nature [3]. Some blue copper proteins of a relatively low molecular-weight, 10–20 kDa, contain only a single copper ion binding site (type 1 or T1) and serve as electron mediators, usually between large immobilized, membrane bound proteins. In analogy to a functionally similar group of iron proteins (ferredoxins), they are named cupredoxins. A second group is the blue multi-copper containing enzymes where the blue T1 copper center is one of the redox centers. Sequential one-electron transfer steps take place, *via* the T1 site from the reducing substrate to another copper center, where the oxidizing substrate (*e.g.* O_2 or nitrite) is reduced [4,5]. Thus, specificity and control are exerted by long range electron transfer (LRET) in both types of blue proteins [6]. Here we review mainly our kinetic studies of long range ET (LRET) in single- and multi-copper proteins that were practically all carried out using the pulse radiolysis method.

In addition to being intrinsically interesting research subjects in their own right, blue copper proteins turned out to have several advantageous properties by serving as general model systems for investigating ET within polypeptide matrices: first, the blue copper site has most probably been selected by evolution to experience minimal structural rearrangements upon shuttling electrons between the Cu(II) and Cu(I) redox state (*i.e.* it has a minimal Franck–Condon barrier) [7]. Further, the copper ions are directly coordinated to amino acid residues without any intervening prosthetic groups. Thus, the protein matrix itself is the only medium separating the redox partners.

2. ET theory and pulse radiolysis techniques

2.1. Theory

Rates of ET depend on the energy required for structural changes in the redox centers as well as on solvent reorganization accompanying ET. Moreover, the redox reaction partners in proteins are held in fixed positions and prevented from coming into inner-sphere contact while small molecules exchange electrons in solutions when they are in close, sometimes direct contact. Thus, the distance separating electron-donor and -acceptor is one decisive and well-defined parameter affecting LRET rates.

Several excellent reviews of ET theory are available [8–10]. In the non-adiabatic limit, where the electronic coupling, in the form of a tunneling matrix element H_{DA} is so weak that the probability of proceeding from donor to acceptor near the transition region is $\ll 1$, the rate constant is proportional to the square of H_{DA} [8]:

$$k = \frac{2\pi}{\hbar} H_{DA}^2 \cdot (FC) \tag{1}$$

The semi-classical Marcus equation (2) may be expressed as [8]:

$$k = \frac{2\pi}{\hbar} \frac{H_{DA}^2}{(4\pi\lambda_{TOT}RT)^{1/2}} e^{-(\Delta G^0+\lambda_{TOT})^2/(4\lambda_{TOT}RT)} \tag{2}$$

ΔG^0 is the reaction free energy and λ the nuclear reorganization energy. Since wave functions decay exponentially with distance, the tunneling matrix element, H_{DA} will decrease with the distance, $(r - r_0)$, as:

$$H_{DA} = H_{DA}^0 \cdot e^{-\beta(r-r_0)/2} \tag{3}$$

H_{DA}^0 is the electronic coupling at direct (van der Waals) contact between electron-donor and -acceptor (where $r = r_0$) and the decay rate of electronic coupling with distance is determined by the coefficient, β. For LRET, the coupling is mediated *via* superexchange by the electronic states of the intervening atoms. In a theoretical model, which has proven to be very useful [11,12], the protein medium is divided into small elements linked by covalent bonds, hydrogen bonds, and through-space contacts, which define an ET pathway. In an extension of this static pathway model for biological ET which is employed here, the influence of structural fluctuations on the kinetics has recently been analyzed in detail and included in the theoretical model [12(b)].

Beta-sheet proteins, composed primarily of extended polypeptide chains interconnected by hydrogen bonds, give rise to ET pathways along the peptide backbone. Many studies have demonstrated that the distance decay constant, β, is $\sim 10\,nm^{-1}$ [13]. Experimental evidence supports the notion that metal-to-metal distances are appropriate for calculating ET rates [9] and this is the length scale employed here.

2.2. Pulse radiolysis

Our studies, reviewed here, employed primarily pulse radiolysis (PR), a method where solvent molecules are subjected to short (0.1–1 μs) pulses of high energy accelerated electrons (~2–10 MeV). Water molecules undergo conversion mainly into OH radicals and hydrated electrons (e_{aq}^-). These primary, rather non-selective reducing or oxidizing agents, may be converted into less reactive and more selective reducing agents such as the CO_2^- radical ($E^0 = -1.8$ V *vs.* SHE) [14] by the following sequence of reactions: hydrated electrons are converted into an additional equivalent of OH radicals in N_2O saturated solutions by the reaction:

$$e_{aq}^- + N_2O + H_2O \rightarrow N_2 + OH + OH^- \tag{4}$$

OH radicals then react with formate anions by H atom abstraction to produce the CO_2^- radical in a diffusion-controlled process:

$$HCO_2^- + OH \rightarrow H_2O + CO_2^- \tag{5}$$

Other reducing and oxidizing radicals such as the uncharged 1-methylnicotinamide radicals (1-MNA*) can similarly be produced. The OH radicals are scavenged by *tert*-butanol to produce a relatively inert radical species:

$$OH + (CH_3)_3OH \rightarrow H_2O + CH_2(CH_3)_2OH \tag{6}$$

1-Methylnicotinamide chloride (1-MNA^+Cl^-) reacts with hydrated electrons to produce 1-MNA* with a reduction potential, $E^0 = -1.0$ V *vs.* SHE [14]:

$$1\text{-}MNA^+ + e_{aq}^- \rightarrow 1\text{-}MNA^* \tag{7}$$

The choice of radicals is based on reactivity and specificity as well as on spectral properties allowing monitoring the reaction products. *E.g.*, protein cystine disulfide residues (RSSR) are reduced by CO_2^- to produce disulfide radical anions RSS^*R^- that have a distinct and relatively intense absorption band at ~410 nm ($\varepsilon_{410} = 10{,}000\,M^{-1}\,cm^{-1}$).

The combination of a wide range of reactivity with time resolution that extends from nanoseconds to minutes, and with convenient spectroscopic monitoring, has made the PR method

highly useful in studies of a wide range of chemical and biochemical ET processes [6,15].

Two main interests have guided our PR studies of redox proteins: elucidation of protein reaction mechanisms and resolution of the parameters that determine the rates of ET within proteins. The fast progress in producing high-resolution 3-D structures of redox active proteins has provided insights that are essential for a meaningful analysis and interpretation of the kinetic results derived from PR studies.

3. Single copper proteins

3.1. Azurins

The T1 copper protein, azurin, contains a Cys3-Cys26 disulfide bridge at a distance of 2.59 nm from the copper ion center (*cf.* Fig. 1). Using sufficiently strong reductants like CO_2^- (*i.e.* $E^0 \leq -1$ V), the disulfide bridge can be reduced to produce a radical anion, RSS*R$^-$, thus providing azurin with a second redox center as indicated in reaction (8) below. The T1Cu(II) center is also reduced directly (9). However, employing an appropriate excess of Cu(II)azurin over the reducing radicals, the intense, transient 410 nm absorption due to the disulfide radical (see above) decays (10) concomitantly with a decrease in the characteristic Cu(II) absorption band at 625 nm ($\varepsilon_{625} = 5700\ M^{-1}\ cm^{-1}$). Process (10) is independent of both protein and RSS*R$^-$ concentrations [16], and is thus an intramolecular RSSR$^-$ to Cu(II) ET.

$$RSSR\text{–}Az[Cu(II)] + CO_2^- \rightarrow RSS^*R^-\text{–}Az[Cu(II)] + CO_2 \quad (8)$$

$$RSSR\text{–}Az[Cu(II)] + CO_2^- \rightarrow RSSR\text{–}Az[Cu(I)] + CO_2 \quad (9)$$

$$RSS^*R^-\text{–}Az[Cu(II)] \rightarrow RSSR\text{–}Az[Cu(I)] \quad (10)$$

An example of time-resolved absorption changes due to these reactions is presented in Fig. 2. Following fast, direct bimolecular reductions of the two redox active centers at 410 nm (8) and at 625 nm (9), the slower intramolecular ET (10) is observed. For wild type *Pseudomonas aeruginosa* azurin, the rate constant of process (10) is $k_{ET} = 44 \pm 7\ s^{-1}$ at pH 7.0 and 25 °C. Specific rates and activation parameters of the intra-protein LRET determined for a large number of different azurins, both wild type and single-site mutants are summarized in Table 1.

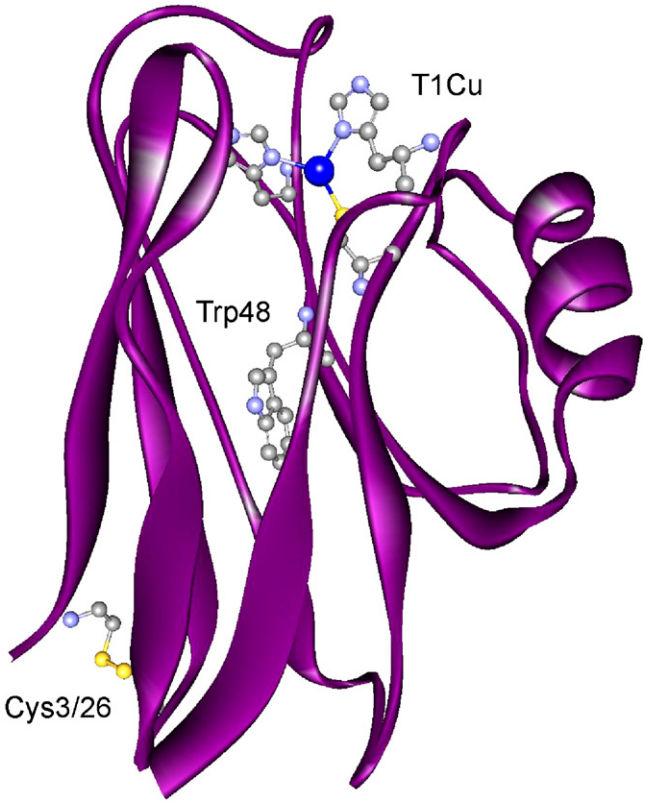

Fig. 1. Three-dimensional structure of *Pseudomonas aeruginosa* azurin. The protein backbone is presented together with the side-chains of three T1Cu ligands, His46, His117, and Cys112. Also shown are Trp48 and the disulfide bridge, Cys3/Cys26. The distance between S_γ of Cys3 and the copper ion is 2.59 nm. Coordinates were taken from the Protein Data Bank, code 4AZU.

Table 1
Kinetic and thermodynamic parameters of intramolecular ET between RSSR and T1Cu(II) in WT and mutated azurins; pH 7.0.[a]

Azurin	k_{298} (s^{-1})	E' (mV)	$-\Delta G^0$ (kJ mol^{-1})	$\Delta H^{\neq}$ (kJ mol^{-1})	$\Delta S^{\neq}$ (J K^{-1} mol^{-1})
Wild type					
P. aeruginosa	44 ± 7	304	68.9	47.5 ± 2.2	−56.5 ± 3.5
P. fluorescens	22 ± 3	347	73.0	36.3 ± 1.2	−97.7 ± 5.0
A. spp.	28 ± 1.5	260	64.6	16.7 ± 1.5	−171 ± 18
A. faecalis	11 ± 2	266	65.2	54.5 ± 1.4	−43.9 ± 9.5
A. denitrificans	42 ± 4	305	69.0	43.5 ± 2.5	−67 ± 9
Mutant					
D23A	15 ± 3	311	69.6	47.8 ± 1.4	−61.4 ± 6.3
F110S	38 ± 10	314	69.9	55.5 ± 5.0	−28.7 ± 4.5
F114A	72 ± 14	358	74.1	52.1 ± 1.3	−36.1 ± 8.2
H35Q	53 ± 11	268	65.4	37.3 ± 1.3	−86.5 ± 5.8
H46G.aq	15 ± 2	<300	<68.5	42.1 ± 3.5	−81 ± 5
H117G.aq	7 ± 3	<300	<68.5	22.0 ± 3.2	−155 ± 11
H117G.im	149 ± 17	240	62.7	54.5 ± 3.9	−22 ± 1
I7S	42 ± 8	301	68.6	56.6 ± 4.1	−21.5 ± 4.2
M44K	134 ± 12	370	75.3	47.2 ± 0.7	−46.4 ± 4.4
M64E	55 ± 8	278	66.4	46.3 ± 6.2	−56.2 ± 7.2
M121H	21 ± 47	215	60.3	28.0 ± 2.1	−127 ± 8
M121L	38 ± 7	412	79.3	45.2 ± 1.3	−61.5 ± 7.2
V31W	285 ± 18	301	68.6	47.2 ± 2.4	−39.7 ± 2.5
W48A	35 ± 4	301	68.6	46.3 ± 5.9	−58.3 ± 6.0
W48F	80 ± 5	304	68.9	43.7 ± 6.7	−61.9 ± 9.7
W48L	40 ± 4	323	70.7	48.3 ± 1.9	−51.5 ± 5.7
W48M	33 ± 5	312	69.7	48.4 ± 1.3	−50.9 ± 7.4
W48S	50 ± 5	314	69.9	49.8 ± 4.9	−44.0 ± 3.5
W48Y	85 ± 5	323	70.7	52.6 ± 6.9	−30.2 ± 3.6

[a] Refs. [16,19].

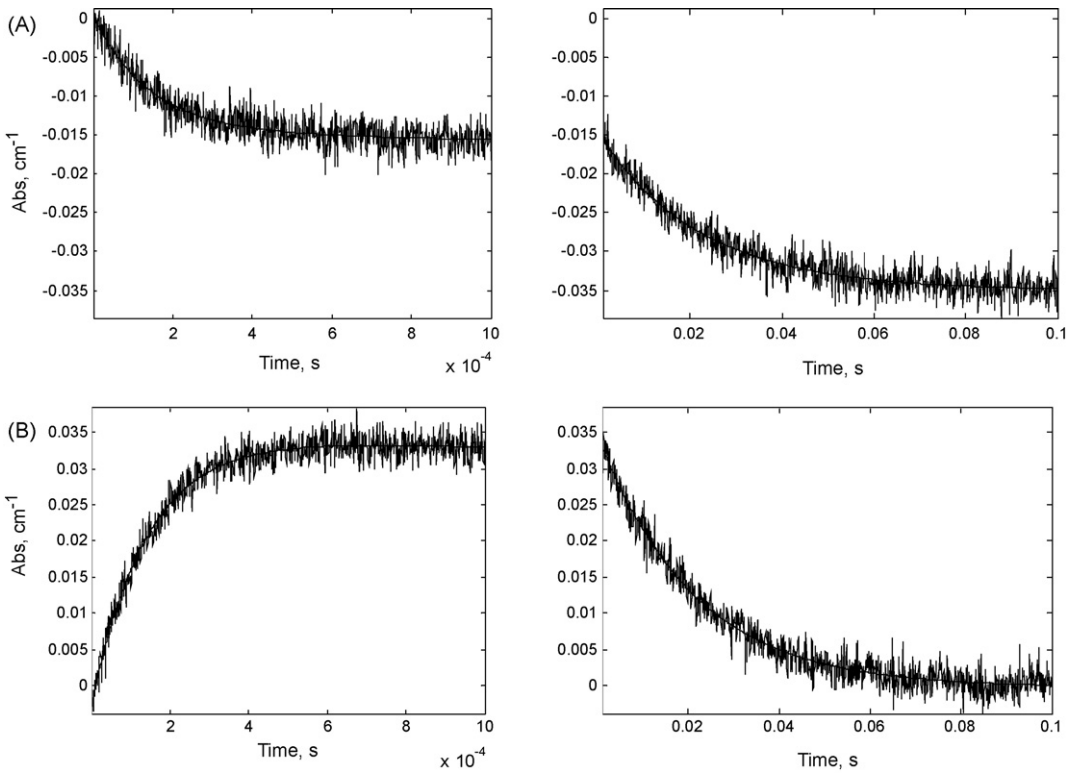

Fig. 2. Time-resolved absorption changes as a result of CO_2^- reduction of *P.a.* azurin [16]. Time is in seconds. A. Reduction of Cu(II) followed at 625 nm. (Left panel) Direct reduction of Cu(II) by the radicals. (Right panel) Indirect reduction of Cu(II) by intramolecular ET from disulfide radicals (*cf.* 1B). B. Formation (left panel) and decay (right panel) of disulfide radical anions monitored at 410 nm. Protein concentration: 12 μM; temperature 298 K; pH 7.0; 0.1 M formate, 10 mM phosphate, N_2O saturated. Pulse width 0.3 μs, 12.3 cm optical path.

Pathway calculations of the intra-protein LRET were performed using the high-resolution 3-D structures of *P. aeruginosa* azurin and its mutants [16] and predict similar ET routes in all azurins (Fig. 3): one path through the polypeptide chain to the copper-ligating imidazole of His46, and another, shorter path goes through the buried indole ring of Trp48, including a through-space jump and the Cys112 thiolate ligand. The electronic coupling factors are 2.5×10^{-7} and 3.0×10^{-8}, respectively. However, this analysis did not include the electronic interaction between the Cu(II) ion and its ligands. The high degree of anisotropic covalency in the copper coordination site would enhance ET through the Cys112 thiolate ligand [17]. Applying the ligand coefficients of Ψ_{HOMO} in azurin calculated by Larsson et al. [18], it can be estimated that ET through the Cys-thiolate ligand would increase by a factor of ~150 over ET *via* one of the His imidazole ligands. Therefore, pathway calculations adjusted by the anisotropic covalency suggest that the "Trp48 pathway" provides the best electronic coupling between the two redox centers. Since the same LRET pathway from $RSSR^-$ to Cu(II) applies to all azurins studied, the reorganization energy, $\lambda_{TOT} = 1.0 \pm 0.05$ eV, and a value for the decay factor, $\beta = 10.0 \pm 0.5\ nm^{-1}$ could be calculated from all the combined kinetic data and activation parameters [16].

In an azurin mutant where an additional tryptophan, in position #31 (Val31Trp), was introduced, the intramolecular ET rate constant increased 10-fold which could not be rationalized in terms of changes in driving force or reorganization energy. Hence, it most probably reflects an enhanced π-electron coupling provided by the additional aromatic residue [19] and further supporting the notion of an optimal "Trp48 ET pathway". Indeed, aromatic residues are often found in positions where they may enhance the electronic coupling between ET donor and acceptor in several systems probably selected by evolution for efficient electron transfer [19–22].

In order to investigate the distance dependence of the LRET from a disulfide radical ion to Cu(II), another engineered azurin has been employed, namely, a triply mutated protein, Cys3Ala/Cys26Ala/Asn42Cys. Here, a Cys42-Cys42 disulfide bond forms a covalently linked dimer under oxidizing conditions while interference from the native Cys3/Cys26 disulfide bond was avoided [23]. The 3-D structure of the dimer shows that a short intermolecular disulfide links the two azurins and causes a strong steric hindrance for internal rotation of the two subunits (Fig. 4) [24]. The Cys42 to Cu distance in the dimer is 1.28 nm as compared with 2.59 nm for Cys3/Cys26 to Cu in the earlier studies. Previous structural studies of a Cys3Ala/Cys26Ala mutant established that the overall structure of the protein is not changed [25].

Reaction of the intermolecular disulfide bridge with CO_2^- radical anions also produces an RSS^*R^- radical ($k_1 \approx 10^9\ M^{-1}\ s^{-1}$) while no reduction of the blue copper(II) center was observed. Following disulfide reduction, a concentration independent, intramolecular $RSS^*R^- \rightarrow$ Cu(II) electron transfer takes place with a rate constant, $k_2 = 7200 \pm 100\ s^{-1}$ at 25 °C and pH 7.0 [23]. The rate constant is in reasonable agreement with calculations using the Beratan and Onuchic [11] tunneling pathway model from S_γ of Cys42 to N_δ of His46, one of the copper ligands (Fig. 4). The 1.28 nm pathway consists of 17 covalent bonds which lead to a calculated rate constant of $4 \times 10^4\ s^{-1}$ at 298 K, which is five-fold larger than the experimentally observed rate. Though not an unreasonably large discrepancy, the following rationale may be considered for this divergence: in wild type (WT) *P. aeruginosa* azurin the ET pathway includes S_γ of Cys112, while tunneling from the external Cys42/Cys42 disulfide bridge to the copper center proceeds *via* N_δ of His46. The high degree of anisotropic covalency of the copper coordination by the Cys112 thiolate in the blue Cu(II) center [17,18] was pointed out above. Thus, in contrast to 50% of the electron density concentrated

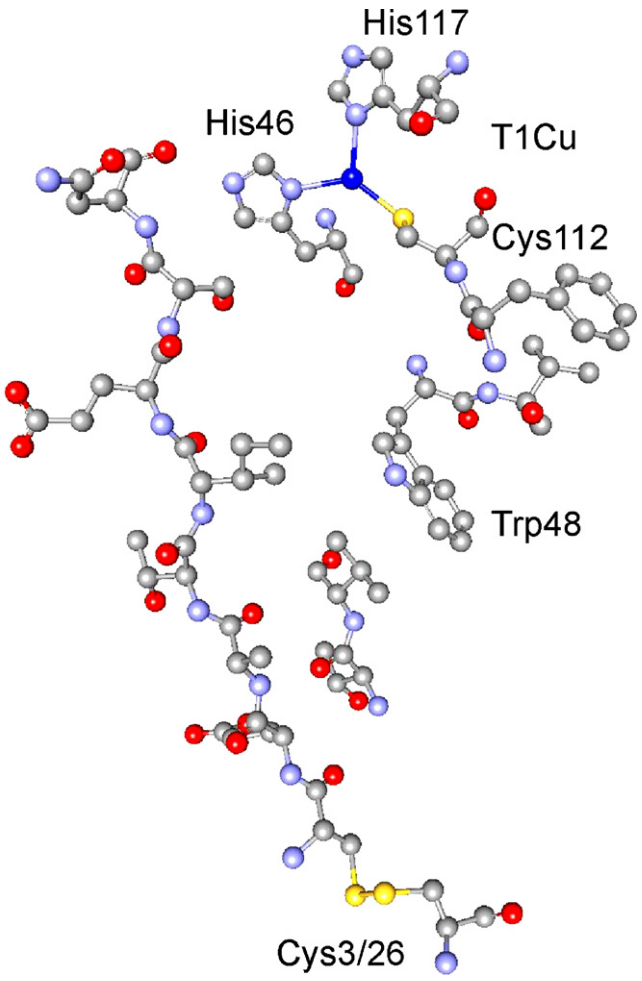

Fig. 3. Suggested ET pathways in *P.a.* azurin from S_γ of Cys3 to T1Cu(II) calculated by the Beratan and Onuchic model [11,12]. The left path depicts a series of covalent bonds followed by a H-bond to the copper ligand, His46. The right path passes through Trp48 (*cf.* text) and includes a through-space jump and two hydrogen bonds.

on the Cu–S bond, only 4% is present on each of the ligating imidazoles. This would drastically diminish the electronic coupling in the dimer compared with WT azurin and cause the observed lower rate.

Comparison of the activation parameters determined for the azurin dimer as well as for related blue copper containing enzymes (*cf.* next section) with those obtained for monomeric azurins provides an additional noteworthy observation: in all azurins (except for the dimer), the RSS*R$^-$ to Cu(II) LRET is controlled by a relatively large activation enthalpy, while in the blue multi-copper proteins, including the present azurin dimer, the activation enthalpies are relatively small (Table 2). In the latter proteins, large negative activation entropies are rate determining, although the connecting ET pathways are considerably shorter. Thus, in the monomeric azurins where the Cys3/Cys26 site is more solvent exposed than the intermolecular Cys42/Cys42 bridge in the dimer major, solvent reorganization may take place upon ET causing the different activation behavior.

Rates of the above intramolecular ET have also been compared in water and deuterium oxide in order to achieve insight into solvent effects on this LRET in azurin [26]. Surprisingly, the kinetic isotope effect, k_H/k_D, is *smaller* than unity (0.7 at 298 K), primarily due to the different activation entropies in H_2O ($-56.5\,J\,K^{-1}\,mol^{-1}$) and in D_2O ($-35.7\,J\,K^{-1}\,mol^{-1}$) suggesting a distinct role for protein solvation. The reduction potential of Cu(II)/(I) is 10 mV more positive in D_2O at 298 K which supports this interpretation. Also, standard entropy changes differ ($-57\,J\,K^{-1}\,mol^{-1}$ in water and $-84\,J\,K^{-1}\,mol^{-1}$ in deuterium oxide) [26] thus making different contributions to the activation entropies. Furthermore, both the nuclear term of the Gibbs free energy and the tunneling factor include isotope effects. A slightly larger thermal protein expansion in H_2O than in D_2O ($0.001\,nm\,K^{-1}$) is sufficient to account for both activation and standard entropy differences. Thus, the effect of differences in driving force and thermal expansion seem to provide the simplest rationale for the observed isotope effect [26] and underscore the important role of solvent in affecting the rates of internal ET in proteins.

Another interesting and important extension of ET studies of azurin is illustrated by investigations of the ET properties of the binuclear Cu_A site. Cu_A serves as the electron uptake center in cytochrome *c* oxidase and nitrous oxide reductase. Its discovery raised a considerable debate regarding the causes for the evolution of multiple forms of copper electron mediation centers. In an azurin mutant, "purple azurin", the ligands forming the T1 copper site have been replaced by residues constituting the Cu_A site of *Paracoccus denitrificans* cytochrome *c* oxidase [27]. The 3-D structure demonstrated a rather close overall structural similarity between the WT blue copper azurin and the engineered "purple" Cu_A azurin [27]. Our studies show that a similar ET takes place between the disulfide bridge and Cu_A as in T1Cu azurin. However, the rate constant of the intramolecular process is almost three-fold faster than for the same process in the WT single blue copper azurin from *P. aeruginosa* ($k_{ET} = 650 \pm 60\,s^{-1}$ *vs.* $250 \pm 20\,s^{-1}$ at 298 K and pH 5.1), in spite of a smaller driving force (0.69 eV for purple Cu_A azurin *vs.* 0.77 eV for

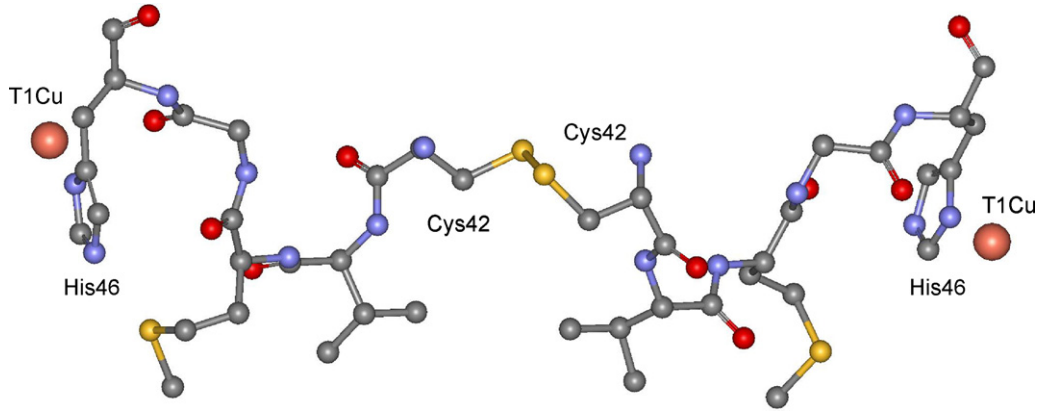

Fig. 4. ET pathway in the dimer azurin Asn42Cys mutant. The two copper ions are connected *via* the coordinating His46 residues and the Cys42/Cys42 disulfide bridge. The Cu–Cys42 S_γ distance is 1.29 nm. The coordinates were taken from the Protein Data Bank, code 1JVO.

Table 2
Comparison of rate constants and activation parameters of internal ET in selected blue copper proteins.

Protein	ET process	k_{298} (s^{-1})	$\Delta H^{\neq}$ (kJ mol^{-1})	$\Delta S^{\neq}$ (J K^{-1} mol^{-1})	ET distance (nm)
P. aeruginosa azurin[a]	$RSSR^- \rightarrow Cu^{2+}$	44 ± 7	47.5 ± 4.0	−56.5 ± 7.0	2.56
P. aeruginosa C3/26A-N42C azurin dimer[b]	$RSSR^- \rightarrow Cu^{2+}$	7200 ± 100	17.7 ± 2.0	−112 ± 6	1.28
A. xylosoxidans CuNiR[c]	T1Cu(I) → T2Cu(II)	185 ± 12	22.7 ± 3.4	−126 ± 11	1.27
Ascorbate oxidase[d] fast step	T1Cu(I) → T2/T3Cu(II)	201 ± 8	9.1 ± 1.1	−170 ± 9	1.22
Ascorbate oxidase[d] slow step	T1Cu(I) → T2/T3Cu(II)	2.3 ± 0.2	6.8 ± 1.0	−215 ± 16	1.22
Rhus laccase[e]	T1Cu(I) → T2/T3Cu(II)	1.1 ± 0.1	14.8 ± 0.2	−211 ± 3	~1.22

[a] Ref. [16].
[b] Ref. [23].
[c] Ref. [53].
[d] Ref. [70].
[e] Ref. [100].

the blue copper center [28]). Thus, the presence of a binuclear Cu_A center as the primary electron uptake site in cytochrome *c* oxidase, illustrates an evolutionary selection of a redox center that is better suited for the biological function.

Reorganization energies of electron-donor and -acceptor sites in a large number of Ru(II) modified *P. aeruginosa* azurins have been determined by Di Bilio et al. [29]. For the T1 copper center, λ_{T1} = 0.82 eV was reported and a λ_{CuA} = 0.4 eV could now be calculated from the observed rate of intramolecular ET in purple azurin [30], *i.e.*, half the reorganization energy required for the blue copper site, supporting the notion that Cu_A is indeed a redox center with improved ET properties, this being mainly a result of the low reorganization energy of the mixed-valence [Cu(1.5)–Cu(1.5)] site.

As the above data clearly illustrate, azurin has turned out to be a very useful model system in studies of the different parameters that control LRET rates in proteins. Specific and well-defined structural changes introduced by single-site mutations have provided a better understanding of the impact of driving force, reorganization energy, as well as chemical nature and structure of the medium separating the redox centers. The ET reactions are well described within the framework of Marcus theory [8] combined with the electronic coupling model developed by Beratan and Onuchic [11]. The experience obtained through studies of ET in azurins has been exploited in further studies on multi-copper enzymes, which is the subject of Section 4.

3.2. Stellacyanin

Stellacyanin, isolated from the sap of the *Rhus vernicifera* tree, is another member of the single blue copper proteins, but unlike azurin, it does not contain a solvent exposed disulfide. However, stellacyanin contains two free histidine residues (His32/100) which according to our model calculations [31] are surface exposed and separated from the T1 center by ~1.8 nm. Winkler et al. have employed ruthenium complexes that coordinate surface exposed imidazole residues [32], thereby constructing semi-synthetic systems containing two or more redox centers which were then amenable to studies of the impact of intra-protein LRET rates on the separation distances between the reacting sites. Indeed, both free histidines on stellacyanin became labeled by pentaammineaquaruthenium(III) [33], and intramolecular ET from pulse radiolytically reduced Ru(II) to T1Cu(II) [34] was studied.

$$Ru(II)Cu(II) \rightleftarrows Ru(III)Cu(I) \quad (11)$$

Since the concentration of the labeled protein was in large excess over the reducing CO_2^- radicals, not more than one Ru(III) center was reduced in each pulse. The observed rate constant of the intramolecular process in ruthenium modified stellacyanin is 0.07 ± 0.01 s^{-1} at 298 K. The temperature dependence and both standard thermodynamic and activation parameters were determined. The reduction potential of $Ru(NH_3)_5His32/100^{3+/2+}$ was measured by non-isothermal cyclic voltammetry to be 61 ± 8 mV at 298 K [34]. Since the reduction potential of the T1 center in stellacyanin is 184 mV at 298 K and pH 7.0 the driving force for the 0.18 nm intramolecular Ru(II) to Cu(II) ET is 0.12 eV. The activation parameters for the process are $\Delta H^{\neq}$ = 19.1 ± 3.1 kJ mol^{-1} and $\Delta S^{\neq}$ = −201 ± 40 J K^{-1} mol^{-1} [34]. The slow ET rate is remarkable and is partially due to the relatively long distance. It is noteworthy that the driving force, 0.12 eV is smaller than that determined for other ruthenium redox proteins studied so far. In azurin, modified with Ru(II) at His83, the rate constant for intramolecular ET from Ru(II) to Cu(II) is 1.9 s^{-1} at 298 K with a driving force of 0.28 eV [35]. Most probably, it is the combination of relatively long separation distance with a small driving force that leads to the unusually low rate of intramolecular ET in Ru-modified stellacyanin.

4. Multi-copper enzymes

The wide range of copper containing enzymes includes two families that contain the T1 site: the multi-copper oxidases (MCOs) and the copper containing nitrite reductases. The former stands out among all copper containing enzymes for being the better known and understood in terms of structure and mode of action. At least two reasons led to this situation: first, their exceptionally wide presence in biological systems and exceptional diversity of functions. Second, MCOs have been used as a model for biochemical reduction of dioxygen to water with its fundamental and applied possibilities. Recent years have yielded a wealth of both genomic sequence data and 3-D structures for different members of the MCO family which have provided insights into both evolutionary and functional features that enable understanding links among members of the MCO family as well as to other blue copper proteins [36]. MCOs are composed of multiple cupredoxin domains, and both two-, three-, and six-domain variants have been identified. The two-domain MCOs (2dMCOs) were hypothesized to be a result of a single cupredoxin domain duplication event and to have architectures resembling the homotrimeric two-domain NiRs which contain a T1 site in each domain 1 and a non-blue type 2 (T2) copper site at the inter-subunit interfaces between domains 1 and 2 [36–39]. Three-domain MCOs (3dMCOs) include ascorbate oxidase, laccases, CueO, and Fet3. The T1 site is located in the C-terminal cupredoxin domain of the latter enzymes, and a three copper nuclear cluster (TNC) comprises a T2 copper and type 3 (T3) copper pair which in the oxidized state is antiferromagnetically coupled. The TNC is located at the interface between domains 1 and 3 [40,41]. Ceruloplasmin is a six-domain MCO, which has three T1 sites, one in each domain 2, 4, and 6 and a T2/T3 cluster between domains 1 and 6 [42].

Several models for the evolution of three- and six-domain MCOs have been proposed. The key evolutionary intermediates of these models are two-domain ancestral MCOs [36–38]. Genome sequence analysis led Nakamura et al. to predict three types of

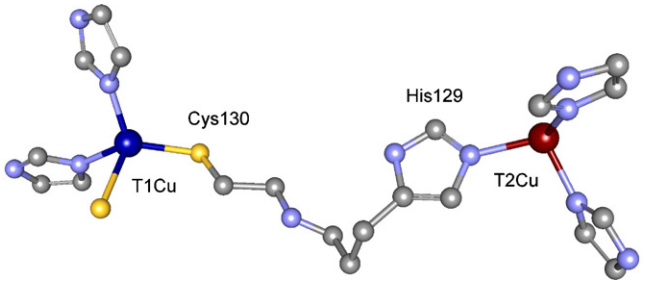

Fig. 5. ET pathway between T1- and T2-copper sites in the blue CuNiR from *Alcaligenes xylosoxidans*. The short path consists of the T1Cu ligand, Cys130 and the T2Cu ligand, His129. The distance between the two copper centers is 1.27 nm. The coordinates were taken from the Protein Data Bank, code 1NDT.

two-domain MCOs (2dMCOs) and classify them according to the assumed location of the T1 copper sites [37]. The type A 2dMCOs contain a T1 site in each domain, whereas the type B and type C 2dMCOs contain a single T1 site in the second or first cupredoxin domains, respectively. The latter two types are postulated to have evolved from the type A 2dMCOs [43].

4.1. Copper containing nitrite reductases (CuNiRs)

The dissimilatory copper containing nitrite reductases (CuNiRs) which partake in the bacterial denitrification process of reducing nitrate to dinitrogen [44] constitute an interesting family of copper containing enzymes. The CuNiRs are homotrimers (109 kDa molecular mass) with 2 copper ions per monomer: a T1 (blue, albeit sometimes green) copper site and a T2 center. The enzyme catalyzes the one-electron reduction of nitrite to nitric oxide [45]:

$$NO_2^- + e^- + 2H^+ \rightarrow NO + H_2O \quad (12)$$

While the T1 center serves as electron uptake site from azurin or pseudoazurin [44], binding and reduction of substrate, nitrite, takes place at the T2 site. Hence, internal T1 → T2 ET is an essential part of the catalytic cycle. Further, it has been suggested that the rate of ET is controlled by changes in the T2 reduction potential induced upon nitrite binding [46,47].

3-D structures have been determined for several CuNiRs, and the overall structures appear to be very similar (*cf.* Fig. 5) [45]. Each monomer contains a T1 copper (bound to two histidines, a cysteine, and a methionine) and a T2 copper coordinated to three histidines while the fourth ligand is water molecule in the oxidized state. One of the ligating histidines comes from a different monomer.

Minor differences in the ligand geometry of the T1 site determine whether the protein appears blue (as in *Alcaligenes xylosoxidans* nitrite reductase, AxNiR) [48] or green, due to the presence of an additional strong band at lower wavelength (as in *Achromobacter cycloclastes* nitrite reductase, AcNiR) [49]. The blue NiRs exhibit an axial EPR signal as in plastocyanin and azurin, in contrast to the rhombic EPR signals of the green NiRs. Although the T1 center of green AcNiR exhibits the "classic" coordination sphere of a T1 site with an axial S(Met), the distortion of the site weakens the Cu–S(Cys) bond, which causes increased absorption around 450 nm, changing the color from blue to green [50].

Kinetic studies have been performed on both AxNiR and AcNiR using either CO_2^- or 1-MNA* radicals as electron donors [51–55]. The first PR experiments of Suzuki et al. [51,52] demonstrated that the T1Cu(II) site is the primary electron uptake site in both the blue AxNiR and green AcNiR, followed by a slower unimolecular reoxidation process that was assigned to intramolecular equilibration between T1Cu(I) and T2Cu(II) (Eq. (13)). The rate of internal ET from T1Cu(I) to T2Cu(II) in AcNiR was 1400 s^{-1}, while in AxNiR ET, $k = 1900\ s^{-1}$ at pH 7.0 [51,52]. The temperature was not reported. In later PR studies using the same reducing radicals, the internal ET kinetics were examined over an extended temperature range, allowing determination of the activation parameters of the internal LRET [53–55]. Rate constants and driving forces for the internal ET in these enzymes are given in Table 3.

$$T1Cu(I)T2Cu(II) \underset{k_b}{\overset{k_f}{\rightleftarrows}} T1Cu(II)T2Cu(I) \quad (13)$$

EPR, EXAFS, and UV–visible spectroscopic studies of reduced and oxidized AxNiR demonstrated that enzyme reduction by ascorbate/phenazine methosulfate, in the absence of nitrite, results in loss of the coordinated water molecule from the T2Cu(I) ion and changing its coordination geometry from near tetrahedral $(His)_3–H_2O$ to trigonal $(His)_3$ [56]. Thus, structural differences between the two redox states of the T2 site would cause a major change in both its reduction potential and reorganization energy compared with those of the T1Cu, where very minor changes in geometry were associated with a change in redox state [57,58].

Very short covalent ET pathways linking the T1 and T2 sites were resolved in the 3-D structures which show that in both blue and green CuNiRs, the paths consist of the T1Cu ligand Cys130 and the neighboring His129 ligand of T2Cu (AcNiR numbering) and a Cu–Cu distance of 1.27 nm distance between the two Cu ions (Fig. 5). This pathway is reminiscent of the link between T1 and the trinuclear site in blue oxidases (see below), thus being a structural feature shared by both families of multi-copper enzymes. Studies of bond-mediated electron tunneling in modified iron-sulfur proteins where electron-donor and -acceptor are separated by a similar Cys-His bridge demonstrated essentially activationless coupling-limited rate constants, *i.e.*, $k_{MAX} \sim 2 \times 10^7–2 \times 10^8\ s^{-1}$ [59].

Despite a smaller driving force, the LRET rate constant observed in the green CuNiR is higher than in the blue enzyme (Table 3). This must be due to a difference in reorganization energies which can be calculated by using the activationless rate constants of the iron-sulfur proteins [59] and introducing the rate constants determined for the CuNiRs into Eq. (2). For green AcNiR $\lambda_{TOT} = 1.16 \pm 0.07$ eV, and in blue AxNiR $\lambda_{TOT} = 1.26 \pm 0.08$ eV (Table 3) [55]. Reorganization energies of the blue T1 copper center vary from 0.72 eV in plastocyanin [60] to 0.82 eV in azurin [29]. Comparison of the 3-D structures of T1 sites in azurin, plastocyanin, and (the blue) AxNiR shows similar geometries and metal ligand distances [45]. Thus, we

Table 3
Kinetic and equilibrium data for internal ET in different CuNiRs at pH 7.0.

Protein	k_{298} (s^{-1})	$-\Delta G^0$ (eV)	$\Delta G^{\neq}$ (eV)	$\Delta S^{\neq}$ (meV/T)	λ_{TOT} (eV)	λ_{T1} (eV)
Blue *Ax*NiR[a]	450 ± 30	−0.010	0.32	−1.31 ± 0.11	1.26 ± 0.08	0.77 ± 0.05[b]
k_f/k_b	185/265					
*Ax*M144A[b] *mutant*	440 ± 35	−0.086	0.32	−1.62 ± 0.13	1.10 ± 0.08	0.45 ± 0.07
k_f/k_b	15/425					
Green *Ac*NiR[c]	1030 ± 80	−0.019	0.30	−1.09 ± 0.09	1.16 ± 0.07	0.57 ± 0.07
k_f/k_b	335/695					

[a] Ref. [53].
[b] Ref. [54].
[c] Ref. [55].

can assume that the reorganization energy of the T1 center in the blue AxNiR is in the same range ($\lambda_{T1} = 0.77 \pm 0.05$ eV). The reorganization energy of the T2 copper center can now be calculated to be $\lambda_{T2} = 1.75$ eV which, as expected, is much larger than that calculated for T1. The T2 center is involved in nitrite binding, reduction, protonation, and product release and therefore has to be solvent accessible as shown in the 3-D structures of NiRs [45]. However, the reorganization energy of the T2 copper center is still below values quoted in the literature for low molecular-weight copper complexes: *e.g.*, for $Cu(phen)_2^{2+/+}$ the reorganization energy has been determined to be 2.4 eV [59]. In contrast, the T1 center is buried inside the protein, 0.6 nm below the Connolly surface of the molecule and isolated from the solvent and therefore requires much smaller reorganization energy.

In view of the identical structures of the T2 carrying domains of AcNiR and AxNiR, the respective reorganization energies, λ_{T2} are expected to be equal, allowing calculating from λ_{TOT} a $\lambda_{T1} = 0.57 \pm 0.07$ eV for the distorted green copper center in AcNiR [55]. Thus, the less symmetric, flattened tetrahedral T1 site of the green CuNiR lowers the reorganization energy compared to λ_{T1} of the distorted tetrahedral geometry of a blue T1 site (*cf.* Table 3). It is noteworthy that the latter value is still larger than that calculated for the binuclear (purple) Cu_A center, 0.4 eV, inserted in a purple azurin [28] (*cf.* Section 3). In conclusion, the tetragonal distortion, possibly arising from small shifts in the loop carrying the Met ligand, emphasizes the subtle, yet important, role of the geometric and electronic structure of the T1 site on its ET reactivity [55].

Several mutants of the blue AxNiR have been produced. In one of them, the weaker T1 ligand, Met144, was substituted by a non-ligating alanine, and the 3-D structure was determined [61]. The mutant still maintains ~30% activity compared with the WT enzyme, yet the reduction potential of T1 increased from 240 to 314 mV. This change in driving force caused by the mutation turned out to have a dramatic influence on the kinetics of ET. No direct bimolecular reduction of T1Cu(II) could be observed while the T2Cu(II) gets reduced directly by either CO_2^- or 1-MNA* radicals followed by a T2Cu(I) to T1Cu(II) ET with a rate constant of 425 s^{-1} [54]. The 3-D structure of the M144A mutant shows that as T1Cu has moved 0.3 Å further below the Connolly surface, together with the ligating His139, the T1 site is more protected from solvent compared to WT CuNiR [61]. It has been demonstrated that the His139Ala mutant does not react with the physiological electron donors of CuNiR, azurin or pseudoazurin, establishing that His139 is essential for bimolecular reduction of the T1Cu(II) [62]. Notably, reduction of the *A. xylosoxidans* His139Ala mutant by dithionite/methylviologen also proceeds *via* reaction with the T2Cu(II) site [62] confirming the more limited access to the T1 site.

Results of PR studies of CuNiRs demonstrated that internal ET could be rate determining for catalytic activity. Comparison of the internal ET rates demonstrates that differences in rates may be attained through ligand changes at the T2 site, *e.g.*, by the substrate binding and its reduction as well as by changes in the reorganization energy of the T1Cu(II) center. While ligand changes of the T2Cu modify both driving force and reorganization energy, the electronic coupling is maintained by an ET pathway consisting of the short, direct covalent peptide stretch connecting the electron-donor and -acceptor.

4.2. Multi-copper oxidases

4.2.1. Intramolecular ET in ascorbate oxidase and ceruloplasmin

Determination at high resolution of the 3-D structures of ascorbate oxidase (AO) [63–65] and later on of human ceruloplasmin (hCp) [66] provided the early structural base for the kinetic investigation of MCOs.

The catalytic cycle in AO proceeds like in all other MCOs by a sequential mechanism where single electrons are transferred from the reducing substrate, ascorbate ions, to T1[Cu(II)] while the TNC serves as the dioxygen binding and reduction site. Intramolecular ET from T1[Cu(I)] to T3[Cu(II)] is thus an essential step required for the transfer of the four electrons required for reduction of O_2 to two H_2O molecules.

The pioneering study of AO by pulse radiolysis was carried out by O'Neill et al. [67] using hydrated electrons as well as CO_2^- and nitroaromatic radicals as reductants. Rather low yields of T1Cu(I) were observed using the former two reagents, while a stoichiometric reduction was observed using the latter. Although proposed, no clear evidence for intramolecular ET was presented [67]. In later studies, carried out in dioxygen containing solutions where O_2^- radicals were the reducing agents, support of the intramolecular reaction step was obtained [68]. Under these conditions, as expected, only limited net reduction yields were obtained.

The intramolecular ET from T1[Cu(I)] to T3[Cu(II)] under anaerobic conditions has been studied independently by different transient kinetic methods [69–73]. Photochemically produced lumiflavin semiquinone reduces the T1[Cu(II)] in a fast second order process ($k = 2.7 \times 10^7$ M^{-1} s^{-1} at pH 7.0) followed by partial reoxidation of the T1[Cu(I)] site with a rate constant of 160 s^{-1} [69]. Though the flavin absorption in the near UV region prevented monitoring the changes at 330 nm where T3[Cu(II)] absorbs, the latter process was interpreted as intramolecular ET from T1 → T3. In a PR study using CO_2^- radicals as electron donor, AO reactivity could be monitored at both 610 nm (T1) and 330 nm (T3) [70] (Fig. 6). A bimolecular, diffusion-controlled T1[Cu(II)] reduction (1.2×10^9 M^{-1} s^{-1} at pH 7.0) was observed followed by biphasic T1[Cu(I)] reoxidation (Fig. 6A) and T3[Cu(II)] reduction (Fig. 6B) proceeding with identical and concentration independent rate constants, confirming that intramolecular ET between the T1 and T3 sites takes place in two distinct phases. The phases were well resolved and their rate constants determined as 200 s^{-1} for the faster and 2 s^{-1} for the slower at 298 K [70]. The temperature dependence of the rates gave rather low activation parameters (*cf.* Table 2). One rationale for the observed two phases could be the presence of active sites differing in reactivity [70]. Some support for this rationale came from the 3-D structure of AO which includes two oxygen ligands at the trinuclear center [64], and protonation equilibrium of these ligands could lead to states with distinct reactivities. Similar results emerged from a later PR study using different organic radicals as reductants yet monitoring only the 610 nm chromophore [71].

The structure of MCOs has most probably been evolutionary optimized for intramolecular ET in the catalytic cycle, and AO has therefore been considered as a model system for investigating the parameters that control intra-protein ET. This raised, several interesting questions: does the internal ET rate depend on the number of reduction equivalents taken up by the molecule, as observed for SLAC discussed below? Is the rate of ET related to the conformational changes the TNC undergoes upon reduction? How does the presence of dioxygen influence the internal ET rates (*i.e.* by affecting the driving force or by an allosteric mechanism)? These questions gain further importance since steady-state kinetic measurements of AO activity yield turnover numbers of 12,000–15,000 s^{-1} [74,75] which are considerably faster than the above rate constants determined for the intramolecular T1 to T3 ET assumed to be the rate-limiting step of the catalytic cycle.

The identical intramolecular ET rate constants, obtained in experiments starting with the fully oxidized enzyme and ending with less than 5% oxidized T1 sites, ruled out the possibility that AO molecules reduced to different degree may exhibit distinct reactivities [70]. Further, no difference in the internal ET rate constants was resolved between enzyme preparations that were examined

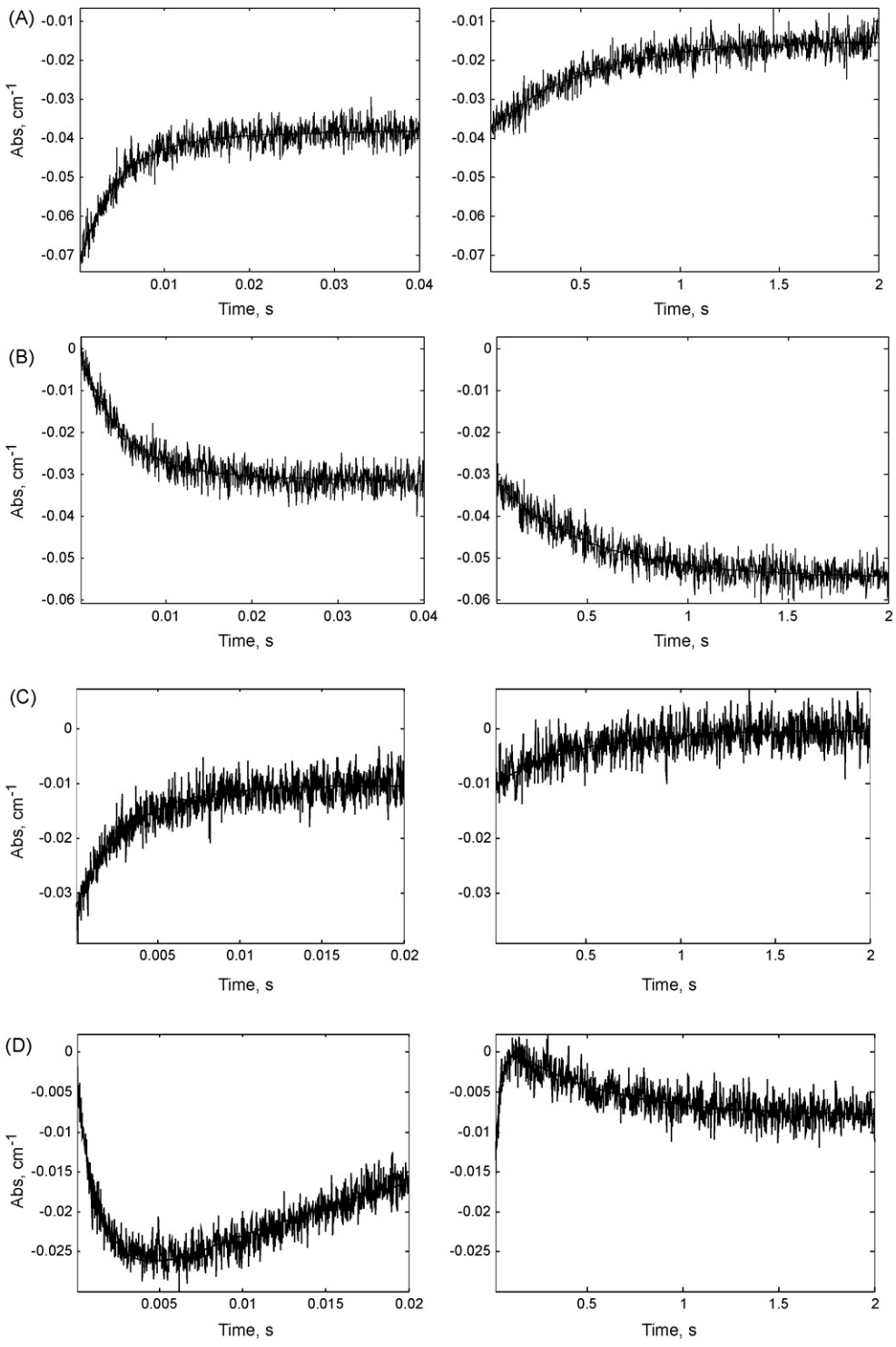

Fig. 6. Time-courses of Zucchini ascorbate oxidase reduction by pulse radiolytically produced CO_2^- radicals under (A and B) anaerobic, N_2O saturated [70] and (C and D) aerobic conditions: $pN_2O = 0.95$ bar; $pO_2 = 0.05$ bar [76]. Protein concentration 5.5 μM; temperature 293 K; pH 5.8; 0.1 M formate. Pulse width 0.5 μs, 12.3 cm optical path length. Time is in seconds. (A and C) Monitored at 610 nm; (B and D) monitored at 330 nm.

as isolated or "activated", ("pulsed") by turning over 1 mM ascorbate in the presence of 0.25 mM O_2 prior to the determination of the intramolecular ET processes. Tollin et al. [72] have observed that freezing and thawing AO solutions may cause biphasic kinetics which are also correlated with a lower enzymatic activity of such samples, yet turnover could restore the "high activity" form which therefore also ruled out functional significance of these findings.

While most of our PR studies were performed under anaerobic conditions, we have also carried out experiments on AO solutions containing controlled low concentrations of O_2 (15–65 μM) that have resolved conspicuous differences in reaction patterns [76] (Fig. 6C). An additional fast intramolecular ET to the TNC was discovered which strictly depended on the presence of dioxygen. The electrons transferred to T3Cu(II) have gradually led to the production of a transient absorption band in the near UV

range ($\lambda_{max} \sim 330$ nm) (Fig. 6D). This is most probably due to the formation of an enzyme-bound oxygen intermediate coordinated to TNC following the above intramolecular ET from T1[Cu(I)] to T3[Cu(II)] and reflects interaction between the partially reduced TNC and dioxygen. Such transient absorptions were first observed for ceruloplasmin [77] and later also in *Rhus* laccase [78–86]. The rate constant of the fast intramolecular ET phase in AO, observed only in the presence of O_2 and monitored at both 610 nm (T1) and 330 nm (T3), was 1100 s^{-1} (293 K, pH 5.8), and was maintained at this value as long as dioxygen remained in the solution [76]. Oxygen intermediates coordinated to the TNC are expected to increase the driving force of the intramolecular ET significantly which does indeed result in the observed higher ET rate. Calculations show that a 100 mV increase in the reduction potential of the T3 center would lead to the observed enhancement in the intramolecular T1Cu(I) → T3Cu(II) ET rate [76]. A similar behavior may be expected in other MCOs and has been observed in the catalytic reduction of O_2 by cytochrome *c* oxidase [87].

The reorganization energy, λ_{TOT} of the above internal ET process in AO could be calculated by applying Eq. (2) to the respective activation parameters. Using a through-bond distance of 1.2 nm between T1Cu and a T3Cu and an electronic decay factor, $\beta = 10\ nm^{-1}$ for ET in β-sheeted proteins (*cf.* Section 3) gives $\lambda_{TOT} = 1.5$ eV. A similar, relatively large reorganization energy was determined for the LRET in the so-called 'small laccase' (SLAC), discussed below, and may be rationalized in terms of the marked structural changes that take place at the TNC during ET: upon reduction of the T3 site the copper–copper distance increases from 0.37 to 0.51 nm [88] and the antiferromagnetic coupling between the copper pair is disrupted along with expected considerable local conformational change around the trinuclear site. The observed maximal rate constant of 1100 s^{-1} for intramolecular ET in AO is still considerably smaller than the turnover number of ~14,000 s^{-1} [74,75]. Therefore, the rate enhancement by dioxygen coordinated to the trinuclear site is not sufficient to explain the difference between the observed maximal enzymatic activity and the T1 → T3 ET rate. However, under optimal conditions, the concentration of reducing substrate is adequate to maintain a steady state of fully reduced copper sites.

The reoxidation of fully reduced AO has been examined by a laser generated triplet state of 5-deaza riboflavin [73]. This experimental approach was limited to monitoring absorption changes of the T1Cu(II). Subsequent to the one-electron oxidation, presumably of the reduced TNC, a rapid biphasic increase in 610 nm absorption was observed which was interpreted as intramolecular ET from T1[Cu(I)] to the oxidized trinuclear center. The rate constant of the faster of the two observed phases (9500 and 1400 s^{-1}, respectively) is comparable to the turnover number for AO under steady-state conditions and renders it very likely to be the rate-limiting step in catalysis.

The 3-D structure of AO determined by Messerschmidt et al. [63–65] has provided the first structural proposal for an effective ET pathway from T1[Cu(I)] to T3[Cu(II)] in MCOs: one of the T1 copper ligands is the thiolate Cys507-(S_γ) while imidazoles of the two neighboring histidines (His506 and His508) coordinate to the T3 copper ions. Thus the path proceeds *via* Cys507 to either His506 or His508 [63] (Fig. 7). Pathway calculations for this ET in AO (*cf.* Section 2.1) supports this notion and further resolve an alternative path *via* a H-bond between the carbonyl oxygen of Cys507 and His506(N_δ). The electronic coupling calculated for the two covalent pathways is 0.010 while for the latter it is slightly higher, 0.014 [70]. A similar effect of the anisotropic thiolate-copper interactions as in the T1Cu site of azurins is presumably also present in AO, enhancing the electronic coupling between Cu(II) and Cys507-(S_γ). Moreover, a similar degree of anisotropic covalency is expected to exist for the more pertinent reduced T1Cu(I) site from which the electrons are transferred intramolecularly in AO [89].

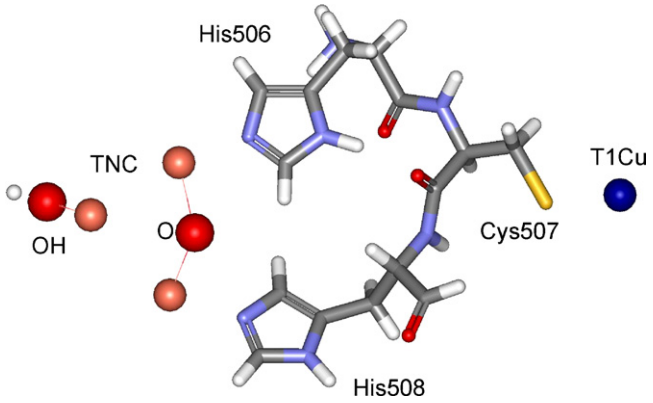

Fig. 7. Intramolecular ET pathway from T1Cu(I) to the TNC in AO. In addition to the two covalent connecting paths, a third path *via* a hydrogen bond between O of Cys507 and N_δ of His506. The direct T1Cu–T3Cu distance is 1.18 nm. The coordinates were taken from the Protein Data Bank, code 1AOZ.

Several features make ceruloplasmin a unique member of the MCO family. Ceruloplasmin is the only known, mammalian member of the MCO family which is found phylogenically all the way to yeast. Its physiological function has finally been established as a ferroxidase, *i.e.*, catalyst of Fe(II) ion oxidation by dioxygen [90]. Human ceruloplasmin (hCp) consists of a single polypeptide with a MW of 132 kDa folded into six cupredoxin domains, each of which consisting of the typical β-sheets (Fig. 8) [66]. Furthermore, three T1 copper sites are present, in domains 2 (T1C), 4 (T1B) and 6 (T1A) whereas the remaining three copper ions form a TNC, bound at the interface between domains 1 and 6. The spatial relation between the TNC and the nearest type 1 (T1A in domain 6) closely resembles that present in laccase and in AO. The three T1 sites are separated by 1.8 nm, a distance which still allows for internal ET at reasonable rates and also increases the probability for electron uptake from reducing substrates. The trinuclear coordination site consists of 4 histidine pairs, two pairs from domain 1 and the other two

Fig. 8. The three-dimensional structure of the six-domains of human ceruloplasmin. Shown are the protein backbone, the position of the three T1 copper ions and the TNC. The coordinates were taken from the Protein Data Bank, code 1KCW.

pairs from domain 6. As in laccases and AO, two of the copper ions are bound to six histidines, typical for the T3 copper pair while the third copper (most distant from T1A) is coordinated to two histidines only, and is designated as the T2 site. In all cases histidine pairs bridge two copper ions and, by analogy to both different laccase and AO structures, an oxygen atom apparently bridges the two T3 coppers while another oxygen is coordinated to the T2 copper ion [66]. Finally, as in the other MCOs, the cysteine thiolate that coordinates to T1A is located in the polypeptide sequence between the two His residues which are bound to the T3 copper pair and provide the by now established ET path between T1 and the TNC.

The reduction potentials of two of the T1 copper centers were determined as 580 and 490 mV, respectively [91]. X-ray absorption spectroscopy established that the resting oxidized hCp contains one permanently reduced T1 center, which means that its reduction potential is at least 1.0 V [92]. Hence, this site cannot be involved in the catalytic process [92]. Based on the 3-D structure of hCp, this high-potential T1 site can be assigned to T1C of domain 2.

In the earliest PR studies of hCp using hydrated electrons as reductants, an internal ET from the initially formed disulfide radical anions to the T1Cu(II) was observed [93]: both the transient absorption of the radicals and the 605 nm band of the T1 Cu(II) site decay in a unimolecular process at an identical rate of $\sim 900\,s^{-1}$. Further slower processes were not investigated.

Later PR studies of hCp demonstrated that CO_2^- radicals also react with surface exposed disulfide groups of the enzyme at diffusion-controlled rates to produce the $RSSR^-$ radicals while no direct reduction of T1 was observed [94]. Rather, T1Cu(II) was reduced by intramolecular ET with a rate constant of $28 \pm 2\,s^{-1}$ at 279 K, followed by a unimolecular electron equilibration between T1Cu(I) and the T2/T3 center. The rate constant $k = 2.9 \pm 0.6\,s^{-1}$ was determined independently by monitoring both T1Cu(II) and T3Cu(II) (Fig. 9). Based on the absorption amplitudes at the former wavelength, the internal ET process equilibrium constant of 0.17 at 279 K has been calculated [94] showing that the electron equilibration between to two sites:

$$T1[Cu(I)]T3[Cu(II)] \rightleftarrows T1[Cu(II)][Cu(I)] \quad (14)$$

is strongly displaced to the left. Thus, after introduction of slightly more than one-electron equivalent into the T1 center, intramolecular ET to the TNC ceased taking place. Nevertheless, a new, slow intramolecular ET from disulfide radicals to another T1[Cu(II)] site was observed, with $k = 3.9 \pm 0.8\,s^{-1}$. Altogether, in these PR experiments carried out under anaerobic conditions, the enzyme took up only slightly more than two electrons.

The first internal electron equilibration step is most probably to the T1A center (*cf.* Fig. 8), since in addition to being proximal to the TNC, this process has only been observed as long as one reducing equivalent is added to the hCp molecules. Furthermore, T1A is most likely the site that possesses the highest reduction potential (580 mV), as in reductive titrations of this enzyme, the first 50% of the total absorption at 610 nm decay within 3 min, while further reduction proceeds much more slowly [91]. The above equilibrium constant of the internal T1–T3 ET equilibration process corresponds to a difference in reduction potential between T1A and T3 of 43 mV, leading to a reduction potential for T3[Cu(II)/Cu(I)] of 537 mV. Finally, identifying T1A as the primary electron acceptor among the T1 centers agrees well with the proposed Fe(II) binding site at Asp1025, which is next to the T1ACu ligating His1026 [41].

Since the ferroxidase site is placed next to several negatively charged acidic residues and is well protected from the solvent by the protein matrix, it is not surprising that only indirect copper reduction by the negatively charged CO_2^- radicals *via* the exposed disulfide groups is observed [94]. This behavior is reminiscent of results of the above PR studies of intramolecular ET in azurins where LRET takes place from the disulfide radical to T1[Cu(II)] over a distance of 2.6 nm (Section 3).

As in all MCOs studied so far, the T1A center is in direct covalent connection with the T3 site providing very efficient electronic coupling. The two pathways consist of nine covalent bonds, with a

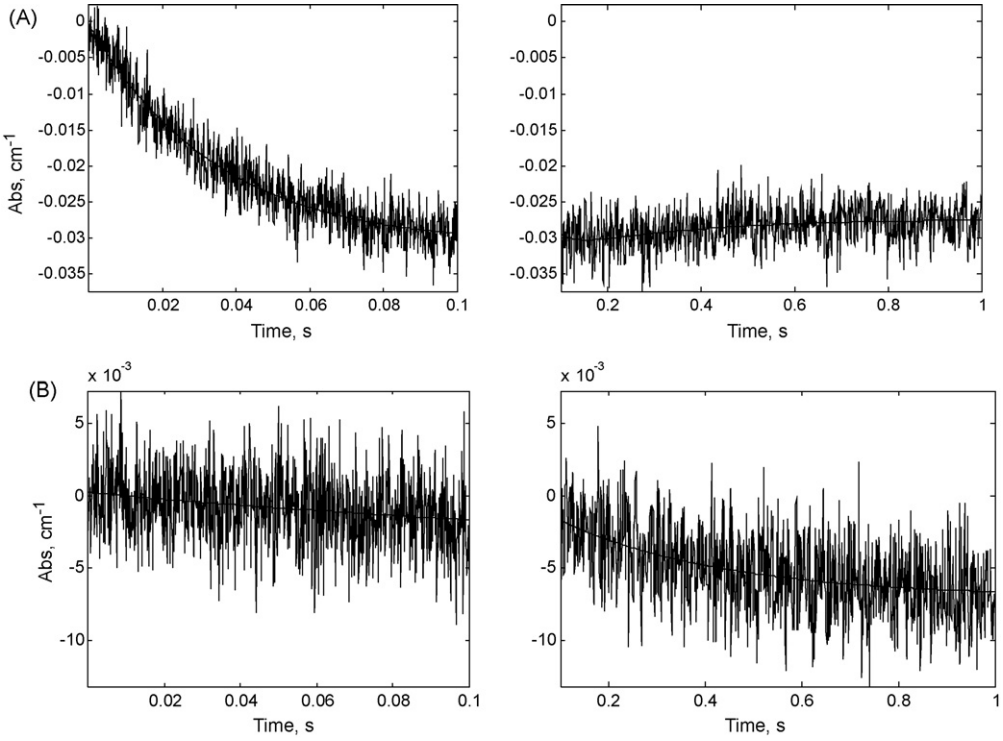

Fig. 9. Time-courses of hCp upon reduction by CO_2^- radicals [94]. Protein concentration 5.3 μM; temperature 279 K; pH 7.0; 0.1 M formate, 10 mM phosphate. Pulse width 0.5 μs, 12.3 cm optical path. Time is in seconds. (A) Reduction and reoxidation of T1Cu monitored at 610 nm; (B) reduction of T3Cu(II) monitored at 330 nm.

direct separation distance between the two copper ions of 1.2 nm. An additional pathway is provided *via* the carbonyl oxygen of Cys, which is hydrogen bonded to a N_δ of a T3 coordinating imidazole (*cf.* Fig. 7). It is noteworthy that this structural arrangement of alternative ET pathways is homologous to the one in laccase and in AO. Similarly, a calculation of the relative electronic coupling between electron-donor and -acceptor gave $\varepsilon = 0.01$, *i.e.*, a very effective coupling further supporting the notion that the T1A copper ion is involved in ET equilibration with the trinuclear site [94]. It is noteworthy that steady-state kinetic measurements of hCp activity with Fe(II) as reducing substrate yield a turnover rate of 2.2 s^{-1} [95], which is similar to the rate constant observed for intramolecular T1 to T3 ET. Intramolecular ET thus seems to be the rate-limiting step also in the catalytic cycle of this enzyme. However, it is worth stressing that all experiments on hCp were performed under strict absence of O_2. Further, the reduction potential of T1A is higher than that of the T3 which could be the reason why only slightly more than two electrons are taken up by hCp under the above conditions [94]. Dioxygen binding to the TNC which under physiological conditions occurs upon reduction of this site, will undoubtedly increase the T3 reduction potential and thus also the driving force for intramolecular T1A[Cu(I)] to T2/T3[Cu(II)] ET. As in all MCOs, ET from reduced T1 copper to the oxygen coordinated trinuclear center is required for the four-electron reduction of dioxygen to water. Finally, the question remains why hCp contains two additional T1Cu centers, which apparently are not participating in the enzyme activity. To answer this, it has been suggested that in addition to being a ferroxidase, hCp may also serve as a copper reservoir in human copper metabolism [73]. Thus, hCp might have two important roles in human metal ion metabolism.

4.2.2. Intramolecular ET processes in laccases

All laccases contain the minimum of four redox active copper ions required for their catalytic activity, the T1 and the TNC comprised by a T2 copper site and a T3 copper pair. High-resolution 3-D structures of several laccases have been determined [96]. The blue T1 Cu(II) ion serves as electron uptake site from its rather diverse substrates, while O_2 undergoes the four-electron reduction to water bound at the TNC. The short through-bond distance from the T1 center to the TNC is 1.2 nm like in AO (*cf.* Fig. 7) and consists of a His-Cys-His peptide sequence with the thiolate coordinating the T1 center while the two neighboring histidine imidazoles coordinate to each of the two T3 copper ions, reminiscent of the peptide bridge connecting the two copper centers in the CuNiRs (*vide supra*).

Some of the key questions concerning the enzymatic mechanism of laccases relate to formation of reaction intermediates during the intramolecular ET between electron-donor and -acceptor sites. The fungal laccase, isolated from *Polyporus versicolor* was one of the first blue copper oxidases to be investigated kinetically by pulse radiolysis [97]. At that early stage, the relatively non-selective hydrated electrons, e_{aq}^-, were still employed and react primarily with aromatic side-chains and disulfide groups to produce transient radicals, some of which decayed in subsequent intramolecular ET steps to the T1Cu(II) center. These reactions were a result of the high reactivity of the e_{aq}^- rather than an indication of physiologically significant ET pathways. Still, these results provided perhaps the earliest evidence for the T1Cu(II) ion being the primary electron uptake site in these oxidases.

Guissani et al. [98] have also performed pulse radiolysis studies on *Polyporus* laccase using several different reagents such as OH, e_{aq}^-, CO_2^- and O_2^- and observed formation of different optical absorption transients. With OH radicals or e_{aq}^-, different reaction products were formed rapidly ($t_{1/2} < 100$ ns) and from the absorption changes in the near UV region it was concluded that OH radicals only react with a limited number of aromatic residues. More complex processes take place between *Polyporus* laccase and e_{aq}^- at diffusion-controlled rates ($\sim 10^{10}$ M^{-1} s^{-1}) with both aromatic and non-aromatic residues but no specific characterization has been pursued [98].

O'Neill et al. [99] have shown that pulse radiolytically produced nitroaromatic radicals reduce the T1Cu(II) sites in tree laccases isolated from *R. vernicifera* and *R. succedanea* in bimolecular processes with rate constants of 2×10^6 M^{-1} s^{-1} and 1.7×10^7 M^{-1} s^{-1}, respectively, at pH 7.4. Significantly, complete reduction of T1Cu(II) in the holoproteins required two reduction equivalents but no further mechanistic details were pursued. The first study of intramolecular ET in a blue MCO was performed on *R. vernicifera* laccase [100]: a rather slow rate of 1.1 s^{-1} at pH 7.0 and 298 K was determined for the T1–T3 electron equilibration, monitored at both 625 nm (T1Cu(II)) and 330 nm (T3Cu(II)). Since no 3-D structural information was available at that time, no further interpretation of this observation could be pursued. However, as for AO, the activation parameters for this ET equilibration are rather low (*cf.* Table 2).

Recently a bacterial small laccase (SLAC) has been isolated from *Streptomyces coelicolor* [101] and reduction kinetics using both CO_2^- and 1-MNA* radicals have been studied [102]. CO_2^- radicals reduce T1Cu(II) on a sub-millisecond timescale, and the observed rate constant depends linearly on protein concentration with a rate constant of $(1.9 \pm 0.2) \times 10^8$ M^{-1} s^{-1} at 25 °C. Time-resolved absorption changes monitored at 590 nm are illustrated in Fig. 10A (left panel). Subsequent to this bimolecular process, partial T1Cu(I) reoxidation takes place with a concentration independent rate constant ($k_{ET} = 8 \pm 1$ s^{-1}, 25 °C in the initial reduction steps; *cf.* Fig. 10A, right panel). Concomitant reduction of T3Cu(II) (Fig. 10B) demonstrates that an intramolecular ET takes place between the T1 and T3 sites. Use of 1-MNA* radicals yielded similar reaction patterns and identical rate constants for the internal ET process [102].

Significantly, by introducing sequential pulses into the SLAC solution, thereby gradually reducing the enzyme, the rate constant of intramolecular ET from T1Cu(I) to T3Cu(II) increases more than 10-fold. Fig. 11 illustrates the observed, slightly sigmoidal increase in the rate constant as a function of the extent of enzyme reduction. However, after the uptake of two electron equivalents, no further ET equilibration was observed, suggesting that fully reduced T3 species is attained at this stage and also that the T2Cu is not involved in this equilibration process. This conclusion is further supported both, by the finding that ascorbate does not reduce T2Cu(II) in SLAC, indicating a low reduction potential for T2Cu (A. Tepper and G.W. Canters, unpublished results) and by simulations of reductive titrations.

Both fresh ("as isolated") SLAC solutions and reoxidized samples (by O_2 after full reduction by the radicals) or by ascorbate

Table 4
Rate constants and activation parameters of intramolecular ET equilibration in SLAC at 298K; pH 7.3.[a]

Enzyme state	k_{ET} (s^{-1})	$\Delta H^{\neq}$ (kJ mol^{-1})	$\Delta S^{\neq}$ (J K^{-1} mol^{-1})
Initial pulse on 'as isolated' enzyme	8 ± 1	25.2 ± 3.2	−142 ± 15
'Cycled' enzyme	15 ± 3 (initial)	9.5 ± 3.7	−189 ± 46
	186 ± 25 (final)	26.2 ± 6.0	−114 ± 18

[a] Ref. [102].

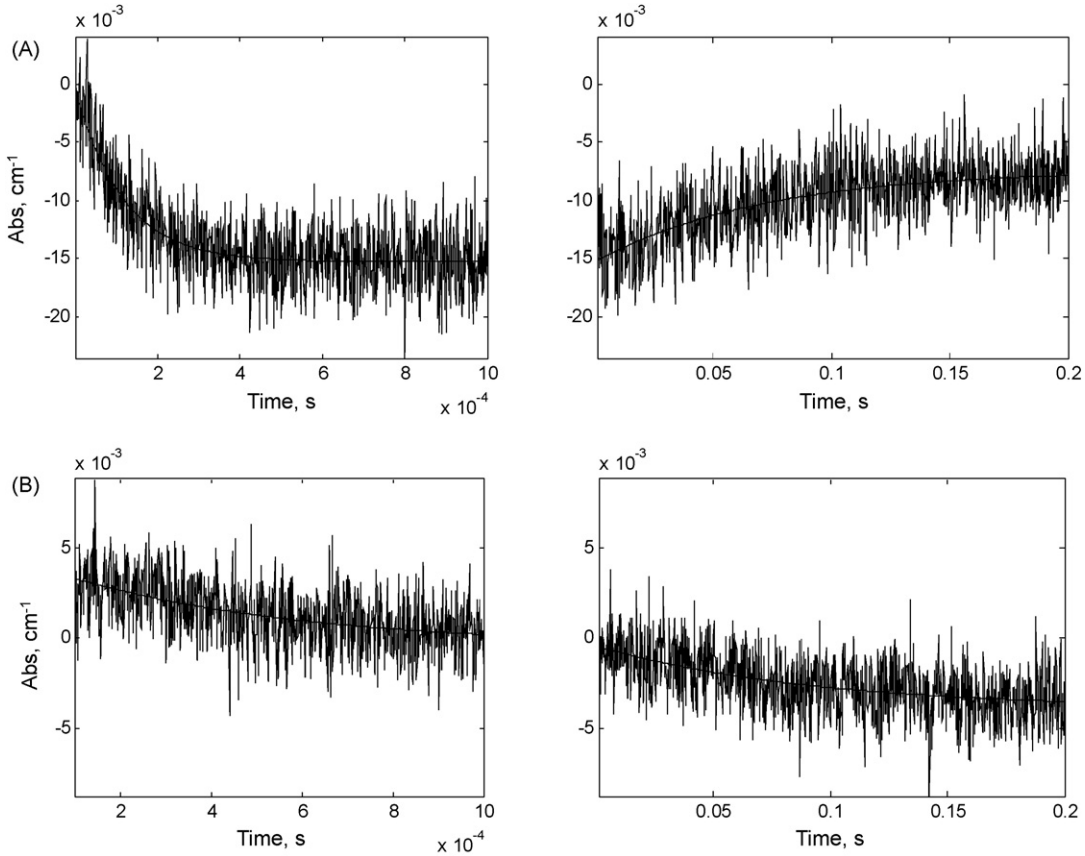

Fig. 10. (A) Time-courses of the SLAC reaction with CO_2^- radicals [102] monitored at 590 nm: initial fast phase of T1Cu(II) reduction (left) is followed by slow reoxidation (right); 23 μM laccase (as isolated); 100 mM sodium formate, 10 mM potassium phosphate, pH 7.3, N_2O saturated solution at 11.5 °C using 1.5 μs pulse length. (B) Time-resolved absorption changes of SLAC monitored at 330 nm: the initial very fast transient (left panel; absorption increase and decrease back to zero) is due to formation and decay of CO_2^- radicals. This is followed by the slower T3Cu(II) reduction (right panel) by intramolecular ET from the T1Cu(I). Conditions are as in Fig. 10A.

("cycled" or "pulsed") exhibited this marked rate enhancement yet the change was larger for "cycled" samples (15–186 s^{-1}). Activation parameters were determined from temperature dependence measurements of the internal ET rates at different states of SLAC activation and reduction (Table 4).

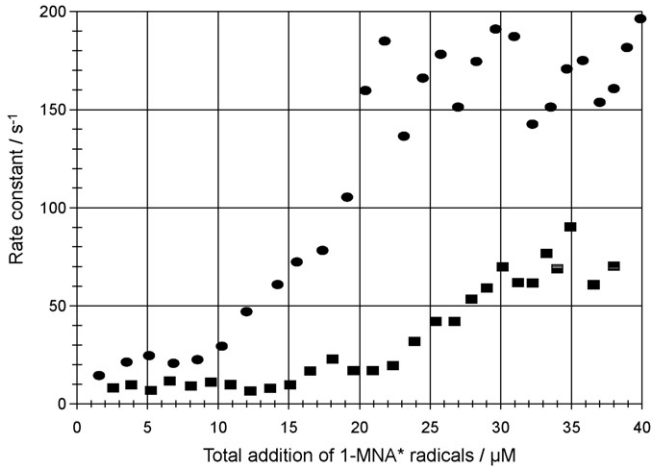

Fig. 11. Observed rate constants of intramolecular T1Cu(I) to T3Cu(II) ET in SLAC as a function of sequentially introducing reduction equivalents to the enzyme (28 pulses, 0.3 μs each) [102]. (■) 22.7 μM "as isolated" laccase, (●) same solution "cycled"; 5 mM 1-MNA, 100 mM *tert*-butanol, 10 mM potassium phosphate, pH 7.3, and 25 °C. Ar saturated, anaerobic conditions.

The following reaction mechanism, independent of the enzyme form was proposed:

$$\text{a.}\quad R^* + T_1{}^{O}T_3{}^{OO} \rightarrow T_1{}^{R}T_3{}^{OO} \rightleftarrows T_1{}^{O}T_3{}^{RO}$$

(internal ET with initial rate) (15)

$$\text{b.}\quad R^* + T_1{}^{O}T_3{}^{RO} \rightarrow T_1{}^{R}T_3{}^{RO} \rightleftarrows T_1{}^{O}T_3{}^{RR}$$

(internal ET with a higher rate) (16)

$$\text{c.}\quad R^* + T_1{}^{O}T_3{}^{RR} \rightarrow T_1{}^{R}T_3{}^{RR} \quad (17)$$

(R^* symbolizes reducing radicals, and the O and R superscripts indicate oxidized and reduced copper centers, respectively).

The marked rate enhancement induced upon reduction could be caused by changes in electron tunneling pathways, in driving force, and/or in reorganization energy. Like in other MCOs, the T1 and the two T3 Cu ions are linked by 11 covalent bonds, and the separating distances are 1.22 and 1.27 nm, respectively [96(f)]. Using an electronic decay factor of 10 nm^{-1} [9] yields an activationless $k_{MAX} = 2.4 \times 10^7\ s^{-1}$. The rate constant for initial reduction phase of the "as isolated" enzyme, 8 s^{-1} corresponds to an activation energy, $\Delta G^{\neq} = 0.378$ eV. The equilibrium constant for reaction (15) is 0.41 at 298 K, equivalent to a driving force, $-\Delta G^0 = -0.023$ eV. Applying the semi-classical Marcus equation (2) [8], a reorganization energy, $\lambda_{TOT} = 1.46$ eV was calculated in good agreement with all previously reported values for this ET [9]. The equilibrium constant for reaction (16) is 5.0 (or $-\Delta G^0 = +0.041$ eV). Thus the larger driving force

contributes slightly to a rate increase, but since $|\Delta G^0| \ll \lambda_{TOT}$, the increase in ET rate is dominated by changes in the reorganization energy. A ~20-fold increase in rate constant requires a decrease in $\Delta G^{\neq}$ to 0.32 eV that in turn would require a small (0.2 eV) decrease in λ_{TOT} to 1.3 eV. Thus, the primary cause for lowering the reorganization energy upon reduction could be structural changes in the TNC, either directly in the coordination sphere of the metal ions, or indirectly in the trimeric SLAC quaternary structure, or in both. A semi-reduced T3 center is an obvious transient since ET from T1 to the binuclear T3 proceeds in two separate single electron transfer steps. In AO, the only MCO for which 3-D structure of the reduced state is available, the reduced T3 Cu–Cu separation distance is 5.1 Å as compared to 3.8 ± 0.1 Å in the oxidized state [88]. Similar findings have been reported for T3 copper proteins, including hemocyanin (Hc), tyrosinase (Ty) and catechol oxidase [103]. No 3-D structural data are available for intermediate reduction states of the MCOs. Still, the semi-reduced T3 site ("half-met form") for Hc and Ty has been studied by spectroscopic techniques [104,105]. In *Streptomyces antibioticus* Ty the paramagnetic Cu in the half-met form still carries a hydroxyl (or water) ligand, which is displaced upon substrates binding [105]. The first T1 to T3 electron transfer in SLAC probably leads to uncoupling of the T3 pair and breaking of the linking OH^- bridge, yet not affecting the ET pathway. The structure of a semi-reduced intermediate would thus be closer to that of the fully reduced than to the oxidized state, and cause the observed decrease in λ_{TOT} for the second internal ET step.

Dependence of the intramolecular ET rates on extent of reduction has not been observed in other MCOs, *cf.* above. However, as SLAC belongs to the trimeric MCOs [96(f)], changes in the T3 coordination sphere may not be the only cause for the enhanced reactivity upon reduction. Another likely origin of the observed rate enhancement could be its distinct quarternary structure: since the TNC in SLAC is located at a monomer–monomer interface and each T3 Cu is bound to ligands from two different monomer chains [96(f)], changes in the TNC reduction state could cause changes in the quaternary structure of the trimer (also mediated by the changes in the TNC structure) and thus provide a rationale for the behavior of SLAC. Significantly, in the analogous copper nitrite reductases, which are also homotrimers, evidence has indeed been provided for marked interactions among the monomers [43,106].

Control of internal ET rates by intrinsic site–site interactions is an intriguing functional feature, encountered for the first time in MCOs. The only other known case of such control involving transition metal-based redox catalysis is a negative site–site interaction between the hemes in *P. aeruginosa* and *P. stutzeri* cd_1 nitrite reductases [107]. An enhanced ET reactivity with increasing extent of reduction and the resultant preference for fully reduced T3 observed in SLAC have consequences for the O_2 reduction process: binding of O_2 to $T_1{}^RT_3{}^{RR}$ or $T_1{}^OT_3{}^{RR}$ would yield a peroxy intermediate promoting additional electron uptake by the enzyme before the crucial steps of dioxygen bond splitting and water formation [84]. Moreover, favoring the formation of the fully reduced T3 site over two half-reduced sites provides a possible evolutionary advantage under conditions of limited reducing substrate.

4.2.3. Formation of O_2 intermediates during MCO catalysis

Rates of internal ET processes in MCOs depend on the distribution of reduction equivalents between the different sites and thereby determine the reactivity with dioxygen and the nature of intermediates produced. This, for example, is illustrated above by the dependence of the rate of LRET on the degree of reduction leading to preferential reduction of the T3 site which was interpreted as promoting peroxide formation rather than other intermediates [102]. Further, a major reason for the intense interest in structure and function of MCO is their capacity to catalyze the four-electron reduction of O_2 to water. This is achieved in spite of the relatively high energy barriers and without the release of any intermediates (*e.g.* reactive oxygen species) from the enzymes. The last four decades have provided a very large amount of biochemical, structural, spectroscopic, and kinetic information yet a precise model of the above reaction mechanism is still incomplete. Studies of the reduction half-cycle in MCOs have focused on kinetics of ET to the electron uptake site, T1Cu(II) as well as the internal transfer to the TNC. Results of studying the former step have contributed to establishing the notion that T1 acts as the oxidation site for the diverse physiological substrates [93,97]. Understanding the process of electron distribution from the T1Cu(I) to the other sites is essential for resolving the reduction mechanism of dioxygen and its intermediates [78–86]. Earlier studies have concentrated on *Rhus* laccase, while more recent years have provided additional information, illustrating the situation in related enzymes such as laccases isolated from other sources, including SLAC as well as ascorbate oxidase, ceruloplasmin and its yeast analogue Fet3p.

Our early PR study where *Rhus* laccase could also be reduced by superoxide radicals in aerobic solutions was carried out under conditions where laccase molecules were reduced by only a single electron equivalent [108]. Significantly, from absorption changes monitored at 625 nm, 60–100% reoxidation of the enzyme was observed with a first order rate constant of 2.5 s^{-1} implying that even single equivalent reduced laccase molecules are reactive with O_2. Still, the nature of this reaction product, probably a peroxide adduct of the TNC components has not been determined. It is however noteworthy that the above rate is faster than the T1 to T3 ET rate, illustrating the impact of dioxygen presence on the driving force.

As stated above, a large array of different experimental approaches have been employed in efforts to identify intermediates in the reaction of MCOs with O_2: reaction of the fully reduced enzyme with O_2; reaction of the oxidized enzyme with a reductant in the presence of O_2; and reaction of the oxidized enzyme with partly reduced dioxygen species like hydrogen peroxide or superoxide radicals. Use of fast reaction kinetics, monitoring different spectroscopic probes and the use of oxygen isotopes helped in identifying or suggesting specific intermediates [109]. Other studies have been carried out on modified MCOs, notably on laccase where the copper has been replaced in the T1 site by mercury, producing an essentially inactive enzyme [110].

Along these lines, early detailed analyses of the optical absorption and circular dichroism (CD) spectra of native *R. vernicifera* laccase have been performed [83,84] (*cf.* Fig. 12) following: (a) addition of one equivalent of hydrogen peroxide to oxidized laccase (Fig. 12B, insert); (b) reduction with ascorbate under aerobic conditions; (c) reaction of partial or fully reduced enzyme with O_2 (Fig. 12A); (d) reductive titrations of the peroxo-laccase (Fig. 12B); and (e) oxidative titrations of the reduced enzyme with hydrogen peroxide (Fig. 12B). All results of these studies have corroborated the notion that peroxo-laccase is a *bona fide* distinct and stable intermediate in the catalytic cycle of this enzyme, and probably also of its analogous MCOs [83–86,108].

Long-lived optical changes were observed in the CD spectrum, particularly in the near UV range, upon reaction of partially or fully reduced *Rhus* laccase with O_2 [84]. The characteristic negative Cotton effects suggested that laccase-oxygen intermediates are formed (Fig. 12A) as similar changes are observed when oxidized laccase reacts with one equivalent of hydrogen peroxide (Fig. 12A, insert) [83] which were assigned to the formation of a peroxo-laccase derivative and quantitatively corroborated by the uptake of the expected (6) reduction equivalents! Spectroscopic studies of AO have demonstrated that the oxidized enzyme also binds a stoichiometric amount of hydrogen peroxide to the T3 copper pair as

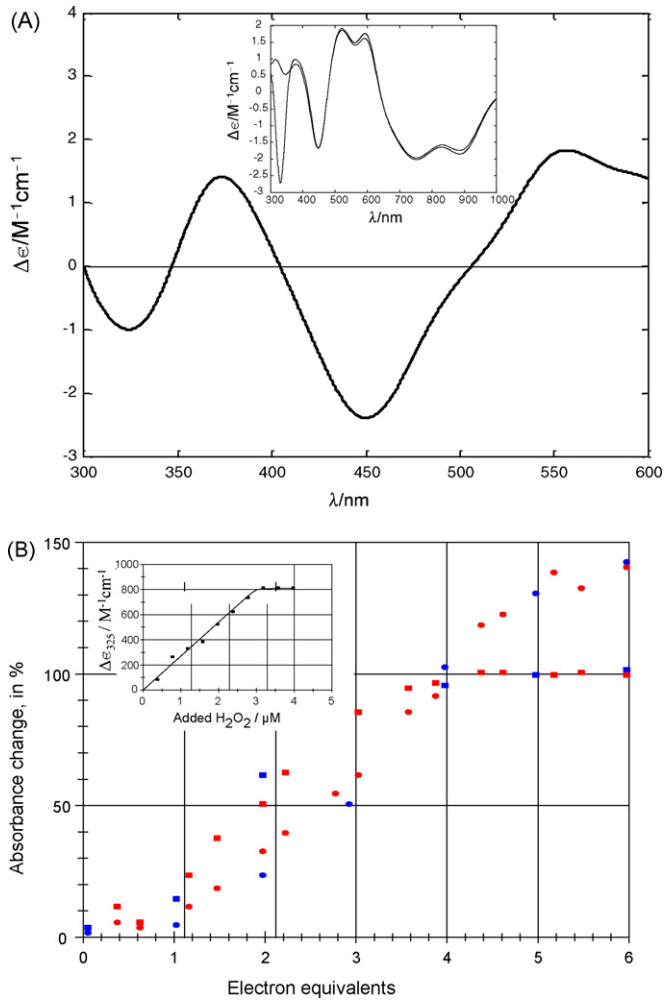

Fig. 12. (A) CD spectrum of partly reduced *Rhus* laccase reacted with O_2 (modified from Ref. [84]). Laccase, 0.09 mM, in 0.1 M phosphate, pH 7.0, 298 K, was reduced with 0.05 mM ascorbate under anaerobic (Ar saturated) conditions followed by reoxidation with dioxygen. Insert: CD spectrum of peroxo-laccase produced by adding 1 molar equivalent of H_2O_2 to *Rhus* laccase, 0.12 mM in 0.1 M phosphate, pH 7.0 (modified from reference [83]). (B) Redox titrations of *Rhus* laccase: to 0.20 mM laccase solution, an equimolar amount of H_2O_2 was added and was left overnight with a trace amount of either catalase or platinum black in order to remove unbound peroxide. After Ar saturation, the laccase solution was reductively titrated with ascorbate (blue points). Upon reaching full reduction, the laccase solution was titrated with H_2O_2 (red points). Squares represent T1 (615 nm) and circles T3 (325 nm) absorption. The absorption values were calculated as $(A - A_{red})/(A_{ox} - A_{red})$ in %, where A is the measured absorbance corrected for dilution, A_{ox} and A_{red} the absorbance of the fully oxidized and fully reduced chromophore, respectively. Insert: titration of oxidized laccase with hydrogen peroxide. To a 3.0 μM laccase solution was added small aliquots of 1.0 mM H_2O_2. $\Delta\epsilon_{325}$ was calculated as the extinction difference between peroxide treated and fully oxidized laccase, corrected for dilution. The curve was calculated using a $K = 1 \times 10^9\ M^{-1}$ (modified from Ref. [82]).

evidenced by the characteristic change of the ~325 nm band [74]. Thus, in view of the close sequence similarity between laccase and AO, the notion of a T3 copper peroxide complex formation by MCOs gains further support. Moreover, the 3-D structure of the peroxide derivative of AO prepared in a similar fashion to the above has been determined. This structure showed that the peroxide binds terminally as HO_2^- end-on to one of the two T3 copper ions [88]. The Cu–Cu distance increases from 0.37 nm in oxidized AO to 0.48 nm, and the bridging oxygen present in the oxidized native enzyme is lost.

It has previously been suggested that the proposed peroxo-laccase formation is caused by oxidation of partly reduced T3 sites present in the resting laccase [110]. However, this has clearly been excluded as only addition of hydrogen peroxide to laccase, already established to be fully oxidized, causes the intensity increase at 325 nm (Fig. 12) and produces the large negative Cotton effect at the same wavelength [83,84]. Further, neither strong inorganic one-electron oxidants nor organic two-electron oxidants cause these changes. In addition, reductive titrations of peroxo-laccase clearly established that six reduction equivalents are required in order to fully reduce this laccase derivative (Fig. 12B). These results are consistent only with observation of a genuine peroxo-laccase product with a long lifetime and a high-affinity formation constant, $K \sim 10^9\ M^{-1}$ [82]. While the sensitivity of laccase to photoreduction has been established [111], it is unclear to what extent the well known reduction caused during different experiments performed by the use of synchrotron radiation has affected the results that did lead to other mechanistic conclusions [110].

Recently the 3-D structure of peroxide bound to the T3 site of another MCO, the Cot A laccase, has also been determined. This structure differs from that observed for AO in having both oxygen atoms coordinated, each to one of the T3 coppers [112]. Other studies, mainly employing theoretical calculations and advanced spectroscopic methods essentially support these conclusions [113]. Thus, the following current model of the initial step of dioxygen reduction is widely accepted, namely that reduced T3 site binds O_2 and produces the first reduction intermediate, a bound peroxide. The next step(s) in this oxidative catalytic half-cycle is far less clear and may even differ in details among MCOs. Thus, already the early studies of *Rhus* laccase oxidation using O^{17} and O^{18} labeled dioxygen have suggested that a single electron reduction step causes breaking of the oxygen–oxygen bond of the bound peroxide intermediate and produces a free radical intermediate [109]. This radical, identified by its oxygen-17 content, was proposed being an O^- which decays in parallel to the appearance of the oxidized T2 copper with a half-life of ~13 s. Significantly, use of oxygen-18 showed that only one water molecule (produced as a result of the three electrons reduction) is released immediately into the bulk solvent. Only upon transfer of the fourth electron to the T2 bound radical is the second water molecule produced, yet remains bound to that site for a relatively prolonged time [109].

The above evidence suggesting a role for T2 copper in the O_2 reduction led to an examination of T2Cu(II) on NMR line-width in O^{17} enriched water [114]. Results have clearly supported the observations of Brändén et al. [109], further illustrating the coordination model of the T2 site and the notion that oxygen atoms are transferred in a controlled fashion from the reduction site, T3 to the T2 copper from which they dissociate rather slowly [114].

During the last decades more studies have addressed the dioxygen reduction mechanism by MCOs. While the formation of a T3 bound peroxide as the first intermediate step (that can also be produced by reaction of the fully oxidized enzyme reacting with H_2O_2, *vide supra*), is widely accepted, several models were proposed for the next steps. One model is based primarily on results of 3-D MCO structures and includes another, probably concomitant, two electron transfer to the bound peroxide, causing O–O bond cleavage and protonation, followed by formation of a hydroxide bridge between the two T3 copper ions and migration of the second oxygen atom to ligate the T2 ion [115].

Significantly, a very recent report by Tepper et al. [116] brings evidence that there might be differences in the final steps of the peroxide reduction among MCOs of diverse sources. Both EPR and optical spectroscopy were employed for investigating the products of dioxygen reduction by the small laccase, SLAC isolated from *S. coelicolor*. Using either WT or a T1 mutated SLAC derivative, the formation of a free radical derived from an amino acid side-chain (probably Tyr108) of the enzyme has been observed. Specifically, it was suggested that out of the four electrons required for the

formation of two water molecules, one is provided from the latter aromatic residue producing a transient free radical. Since the trimeric (two-domain) SLAC structure differs from the majority of laccases studied so far, and has also been shown (*vide supra*) to exhibit a different pattern of internal ET rate and distribution dependence on the reduction state of the enzyme, it remains to be learned if the above distinct intermediate formed is a singularity or a characteristic of the trimeric 2dMCOs sub-family.

5. Conclusions

This review clearly illustrates that pulse radiolysis is a suitable and rather useful method for studies of ET processes to and within redox proteins, such as the blue copper proteins discussed here. The two main objectives guiding our studies were (1) to attain a better understanding of the intramolecular electron transfer process in the polypeptide matrix separating the redox centers and (2) to resolve the detailed reaction mechanisms of the proteins, including the catalytic cycles, assumed to be a result of evolutionary selection.

Structure–function relations of a diverse group of electron mediating proteins with both natural (*i.e.* wild type) and artificial (*e.g.* mutations) structural features have been discussed. The review thus provides an interesting illustration of evolution's profound impact on development and selection of ET sites and pathways, thereby adjusting the rates to requirements of specific reactions. Clearly, several parameters like driving force, distance, and the nature of the medium separating electron-donor and -acceptor contribute to this elaborate control.

Though considerable theoretical studies as well as structure/reactivity analysis have been focused on the blue copper proteins, a deeper understanding of the functional reasons which led to the evolutionary selection of this family is still needed. One major challenge still remains, as the mechanism by which dioxygen reduction to water takes place is still only partially resolved.

Acknowledgements

OF wishes to thank the generous support, extended by the Kimmelman Center for Biomolecular Structure and Assembly at the Weizmann Institute of Science. We are deeply indebted to Dr. Scot Wherland for his thorough review of the manuscript and numerous thoughtful suggestions which have caused major improvement of this review.

References

[1] K.D. Karlin, Z. Tyeklar (Eds.), Bioinorganic Chemistry of Copper, Chapman & Hall, New York/London, 1993.
[2] A. Messerschmidt, R. Huber, T. Poulos, K. Wieghardt (Eds.), Handbook of Metalloproteins, vol. 2, J. Wiley and Sons, 2001.
[3] R. Lontie (Ed.), Copper Proteins and Copper Enzymes, CRC Press, 1984.
[4] C. Ostermeier, S. Iwata, H. Michel, Curr. Opin. Struct. Biol. 6 (1996) 460.
[5] A. Messerschmidt, in: K.D. Karlin, Z. Tyeklar (Eds.), Bioinorganic Chemistry of Copper, Chapman & Hall, New York, 1993.
[6] O. Farver, I. Pecht, Prog. Inorg. Chem. 55 (2007) 1.
[7] H.B. Gray, B.G. Malmström, Comments Inorg. Chem. 2 (1983) 203.
[8] R.A. Marcus, N. Sutin, Biochim. Biophys. Acta 811 (1985) 265.
[9] H.B. Gray, J.R. Winkler, Q. Rev. Biophys. 36 (2003) 341.
[10] J. Jortner, M. Bixon (Eds.), Adv. Chem. Phys. 106 (1999) 35.
[11] D.N. Beratan, J.N. Betts, J.N. Onuchic, Science 252 (1991) 1285.
[12] (a) D.N. Beratan, J.N. Onuchic, J.R. Winkler, H.B. Gray, Science 258 (1992) 1740; (b) D.N. Beratan, S.S. Skourtis, I.A. Balabin, A. Balaeff, S. Keinan, R. Venkatramani, D. Xiao, Acc. Chem. Res. 42 (2009) 1669.
[13] R. Langen, I.J. Chang, J.P. Germanas, J.H. Richards, J.R. Winkler, H.B. Gray, Science 268 (1995) 1733.
[14] M.H. Klapper, M. Faraggi, Q. Rev. Biophys. 12 (1979) 465.
[15] (a) O. Farver, I. Pecht, FASEB J. 5 (1991) 2554; (b) O. Farver, I. Pecht, in: A. Messerschmidt (Ed.), Multi-Copper Oxidases, World Scientific Publications, 1997, p. 355; (c) O. Farver, I. Pecht, in: J. Jortner, M. Bixon (Eds.), Adv. Chem. Phys. Ser., vol. 107, Wiley & Sons, 1999, p. 555.
[16] (a) O. Farver, I. Pecht, Proc. Natl. Acad. Sci. U.S.A. 86 (1989) 6968; (b) O. Farver, I. Pecht, J. Am. Chem. Soc. 114 (1992) 5764; (c) O. Farver, L.K. Skov, M.v.d. Kamp, G.W. Canters, I. Pecht, Eur. J. Biochem. 210 (1992) 399; (d) O. Farver, L.K. Skov, T. Pascher, B.G. Karlsson, M. Nordling, L.G. Lundberg, T. Vänngård, I. Pecht, Biochemistry 32 (1993) 7317; (e) O. Farver, L.K. Skov, G. Gilardi, G. van Pouderoyen, G.W. Canters, S. Wherland, I. Pecht, Chem. Phys. 204 (1996) 271; (f) O. Farver, N. Bonander, L.K. Skov, I. Pecht, Inorg. Chim. Acta 243 (1996) 127.
[17] E.I. Solomon, R.K. Szilagyi, S.D. George, L. Basumallick, Chem. Rev. 104 (2004) 419.
[18] S. Larsson, A. Broo, L. Sjölin, J. Phys. Chem. 99 (1995) 4860.
[19] O. Farver, L.K. Skov, S. Young, N. Bonander, B.G. Karlsson, T. Vänngård, I. Pecht, J. Am. Chem. Soc. 119 (1997) 5453.
[20] (a) L. Chen, R. Durley, B.J. Poliks, K. Hamada, Z. Chen, F.S. Mathews, V.L. Davidson, Y. Satow, E. Huizinga, F.M.D. Vellieux, W.G.J. Hol, Biochemistry 31 (1992) 4959; (b) A.P. Kalverda, S.S. Wymenga, A. Lommen, F.J.M.v.d. Ven, C.W. Hilbers, G.W. Canters, J. Mol. Biol. 240 (1994) 358.
[21] M. Plato, M.E. Michel-Beyerle, M. Bixon, J. Jortner, FEBS Lett. 249 (1989) 70.
[22] H. Pelletier, J. Kraut, Science 258 (1992) 1748.
[23] O. Farver, G.W. Canters, I. van Amsterdam, I. Pecht, J. Phys. Chem. A 107 (2003) 6757.
[24] I.M.C. van Amsterdam, M. Ubbink, L.J.C. Jeuken, M.P. Verbeet, O. Einsle, A. Messerschmidt, G.W. Canters, Chem.–Eur. J. 7 (2001) 2398.
[25] N. Bonander, J. Leckner, H. Guo, B.G. Karlsson, L. Sjölin, Eur. J. Biochem. 267 (2000) 4511.
[26] O. Farver, J. Zhang, Q. Chi, I. Pecht, J. Ulstrup, Proc. Natl. Acad. Sci. U.S.A. 98 (2001) 4426.
[27] M. Hay, J.H. Richards, Y. Lu, Proc. Natl. Acad. Sci. U.S.A. 93 (1996) 461.
[28] O. Farver, Y. Lu, M.C. Ang, I. Pecht, Proc. Natl. Acad. Sci. U.S.A. 96 (1999) 899.
[29] A.J. Di Bilio, M.G. Hill, N. Bonander, B.G. Karlsson, R.M. Villahermosa, B.G. Malmström, J.R. Winkler, H.B. Gray, J. Am. Chem. Soc. 119 (1997) 9921.
[30] O. Farver, H.J. Hwang, Y. Lu, I. Pecht, J. Phys. Chem. B 111 (2007) 6690.
[31] S. Wherland, O. Farver, I. Pecht, J. Mol. Biol. 204 (1988) 404.
[32] J.R. Winkler, A.J. Di Bilio, N.A. Farrow, J.H. Richards, H.B. Gray, Pure. Appl. Chem. 71 (1999) 1753.
[33] O. Farver, I. Pecht, FEBS Lett. 244 (1989) 376.
[34] (a) O. Farver, I. Pecht, FEBS Lett. 244 (1989) 379; (b) O. Farver, I. Pecht, Inorg. Chem. 29 (1990) 4855.
[35] N.M. Kostic, R. Margalit, C.M. Che, H.B. Gray, J. Am. Chem. Soc. 105 (1983) 7765.
[36] L.G. Rydén, L.T. Hunt, J. Mol. Evol. 36 (1993) 41.
[37] K. Nakamura, T. Kawabata, K. Yura, N. Go, FEBS Lett. 553 (2003) 239.
[38] M.E. Murphy, P.F. Lindley, E.T. Adman, Protein Sci. 6 (1997) 761.
[39] K. Nakamura, N. Go, Cell. Mol. Life Sci. 62 (2005) 2050.
[40] N.E. Zhukhlistova, Y.N. Zhukova, A.V. Lyashenko, A.V. Zaitsev, A.M. Mikhailov, Crystallogr. Rep. 53 (2008) 92.
[41] A.B. Taylor, C.S. Stoj, L. Ziegler, D.J. Kosman, P.J. Hart, Proc. Natl. Acad. Sci. U.S.A. 102 (2005) 15459.
[42] P.F. Lindley, G. Card, I. Zaitseva, V. Zaitsev, B. Reinhammar, E. Selin-Lindgren, K. Yoshida, J. Biol. Inorg. Chem. 2 (1997) 454.
[43] T.J. Lawton, L.A. Sayavedra-Soto, D.J. Arp, A.C. Rozenzweig, J. Biol. Chem. 284 (2009) 10174.
[44] W.G. Zumft, Microbiol. Mol. Biol. Rev. 61 (1997) 533.
[45] E.T. Adman, M.E.P. Murphy, in: A. Messerschmidt, R. Huber, K. Wieghardt, T. Poulos (Eds.), Handbook of Metalloproteins, vol. 2, J. Wiley & Sons, New York, 2001, p. 1381.
[46] F.K. Yousafzai, R.R. Eady, J. Biol. Chem. 277 (2002) 34067.
[47] K. Kobayashi, S. Tagawa, Deligeer, S. Suzuki, J. Biochem. 126 (1999) 408.
[48] Z.H.L. Abraham, D.J. Lowe, B.E. Smith, Biochem. J. 295 (1993) 587.
[49] C.L. Hulse, J.M. Tiedje, B.A. Averill, Anal. Biochem. 172 (1988) 420.
[50] E.I. Solomon, R.K. Szilagyi, S. DeBeer George, L. Basulallick, Chem. Rev. 104 (2004) 419.
[51] S. Suzuki, T. Kohzuma, Deligeer, K. Yamaguchi, N. Nakamura, S. Shidara, K. Kobayashi, S. Tawaga, J. Am. Chem. Soc. 116 (1994) 11145.
[52] S. Suzuki, Deligeer, K. Yamaguchi, K. Kataoka, K. Kobayashi, S. Tawaga, T. Kohzuma, S. Shidara, H. Iwasaki, J. Biol. Inorg. Chem. 2 (1997) 265.
[53] O. Farver, R.R. Eady, Z.H.L. Abraham, I. Pecht, FEBS Lett. 436 (1998) 239.
[54] O. Farver, R.R. Eady, G. Sawers, M. Prudêncio, I. Pecht, FEBS Lett. 561 (2004) 173.
[55] O. Farver, R.R. Eady, I. Pecht, J. Phys. Chem. A 108 (2004) 9005.
[56] R.W. Strange, L.M. Murphy, F.E. Dodd, Z.H.L. Abraham, R.R. Eady, B.E. Smith, S.S. Hasnain, J. Mol. Biol. 287 (1999) 1001.
[57] E.N. Baker, J. Am. Chem. Soc. 112 (1990) 7817.
[58] H.B. Gray, B.G. Malmstrom, R.J.P. Williams, J. Biol. Inorg. Chem. 5 (2000) 551.
[59] E. Babini, I. Bertini, M. Borsari, F. Capozzi, C. Luchinat, X. Zhang, G.L.C. Moura, I.V. Kurnikov, D.N. Beratan, A. Ponce, A.J. Di Bilio, J.R. Winkler, H.B. Gray, J. Am. Chem. Soc. 122 (2000) 4532.
[60] A.J. Di Bilio, C. Dennison, H.B. Gray, B.E. Ramirez, A.G. Sykes, J.R. Winkler, J. Am. Chem. Soc. 120 (1998) 7551.
[61] M.J. Ellis, M. Prudêncio, F.E. Dodd, R.W. Strange, G. Sawers, R.R. Eady, S.S. Hasnain, J. Mol. Biol. 316 (2002) 51.
[62] M. Prudêncio, G. Sawers, F.K. Yousafzai, R.R. Eady, Biochemistry 41 (2002) 3430.

[63] A. Messerschmidt, A. Rossi, R. Ladenstein, R. Huber, M. Bolognesi, G. Gatti, A. Marchesini, R. Petruzzelli, A. Finazzi-Agró, J. Mol. Biol. 206 (1989) 513.
[64] A. Messerschmidt, R. Ladenstein, R. Huber, M. Bolognesi, L. Avigliano, A. Marchesini, R. Petruzzelli, A. Rossi, A. Finazzi-Agró, J. Mol. Biol. 224 (1992) 179.
[65] A. Messerschmidt, R. Huber, Eur. J. Biochem. 187 (1990) 341.
[66] (a) V. Saitzev, I. Saitzeva, G. Card, A. Ralph, B. Bax, P. Lindley, J. Inorg. Biochem. 59 (1995) 719;
(b) I. Saitzeva, V. Saitzev, G. Card, K. Moshkov, B. Bax, A. Ralph, P. Lindley, J. Biol. Inorg. Chem. 1 (1996) 15.
[67] P. O'Neill, E.M. Fielden, A. Finazzi-Agró, L. Avigliano, Biochem. J. 209 (1983) 167.
[68] P. O'Neill, E.M. Fielden, L. Avigliano, G. Marcozzi, A. Ballini, A. Finazzi-Agró, Biochem. J. 222 (1984) 65.
[69] T.E. Meyer, A. Marchesini, M.A. Cusanovich, G. Tollin, Biochemistry 30 (1991) 4619.
[70] O. Farver, I. Pecht, Proc. Natl. Acad. Sci. U.S.A. 89 (1992) 8283.
[71] P. Kyritsis, A. Messerschmidt, R. Huber, G.A. Salmon, A.G. Sykes, J. Chem. Soc. Dalton Trans. (1993) 731.
[72] G. Tollin, T.E. Meyer, M.A. Cusanovich, P. Curir, A. Marchesini, Biochim. Biophys. Acta 1183 (1993) 309.
[73] J.T. Hazzard, A. Marchesini, P. Curir, G. Tollin, Biochim. Biophys. Acta 1208 (1994) 166.
[74] A. Marchesini, P.M.H. Kroneck, Eur. J. Biochem. 101 (1979) 65.
[75] P.M.H. Kroneck, F.A. Armstrong, H. Merkle, A. Marchesini, Adv. Chem. Ser. 220 (1982) 223.
[76] O. Farver, S. Wherland, I. Pecht, J. Biol. Chem. 269 (1994) 22933.
[77] T. Manabe, H. Manabe, K. Hiromi, H. Hatano, FEBS Lett. 23 (1972) 268.
[78] L.-E. Andréasson, R. Brändén, B. Reinhammar, Biochim. Biophys. Acta 483 (1976) 370.
[79] R. Aasa, R. Brändén, J. Deinum, B.G. Malmström, B. Reinhammar, T. Vänngaard, FEBS Lett. 61 (1976) 115.
[80] R. Brändén, J. Deinum, Biochim. Biophys. Acta 524 (1978) 297.
[81] R. Aasa, R. Brändén, J. Deinum, B.G. Malmström, B. Reinhammar, T. Vänngaard, Biochem. Biophys. Res. Commun. 70 (1976) 1204.
[82] O. Farver, M. Goldberg, D. Lancet, I. Pecht, Biochem. Biophys. Res. Commun. 73 (1976) 494.
[83] O. Farver, M. Goldberg, I. Pecht, FEBS Lett. 94 (1978) 383.
[84] O. Farver, M. Goldberg, I. Pecht, Eur. J. Biochem. 104 (1980) 71.
[85] M. Goldberg, O. Farver, I. Pecht, J. Biol. Chem. 255 (1980) 7353.
[86] O. Farver, P. Frank, I. Pecht, Biochem. Biophys. Res. Commun. 108 (1982) 273.
[87] M. Brunori, G. Antonini, F. Malatesta, P. Sarti, M.T. Wilson, FEBS Lett. 314 (1992) 191.
[88] A. Messerschmidt, H. Luecke, R. Huber, J. Mol. Biol. 230 (1993) 997.
[89] J.A. Gluckert, M.D. Lowery, E.I. Solomon, J. Am. Chem. Soc. 117 (1995) 2817.
[90] E.D. Harris, Nutr. Rev. 53 (1996) 170.
[91] J. Deinum, T. Vänngård, Biochim. Biophys. Acta 310 (1973) 321.
[92] T.E. Machonkin, H.H. Zhang, B. Hedman, K.O. Hodgson, E.I. Solomon, Biochemistry 37 (1998) 9570.
[93] M. Faraggi, I. Pecht, J. Biol. Chem. 248 (1973) 3146.
[94] O. Farver, L. Bendahl, L.K. Skov, I. Pecht, J. Biol. Chem. 274 (1999) 26135.
[95] L. Avigliano, A. Finazzi-Agrò, in: A. Messerschmidt (Ed.), Electron Transfer Reactions in Multi-Copper Oxidases, World Scientific Publications, Singapore, 1997, p. 251.
[96] (a) V. Ducros, A.M. Brzozowski, K.S. Wilson, S.H. Brown, P. Ostergaard, P. Schneider, D.S. Yaver, A.H. Pedersen, G.J. Davies, Nat. Struct. Biol. 5 (1998) 310;
(b) F.J. Enguita, L.O. Martins, A.O. Henriques, M.A. Carrondo, J. Biol. Chem. 278 (2003) 19416;
(c) K. Piontek, M. Antorini, T. Choinowski, J. Biol. Chem. 277 (2002) 37663;
(d) N. Hakulinen, L.L. Kiiskien, K. Kruus, M. Saloheimo, A. Paananen, A. Koivula, J. Rouvinen, Nat. Struct. Biol. 9 (2002) 601;
(e) T. Bertrand, C. Jolivalt, P. Briozzo, E. Caminade, N. Joly, C. Madzak, C. Mougin, Biochemistry 41 (2002) 7325;
(f) T. Skalova, J. Dohnalek, L.H. Ostergaard, P.R. Ostergaard, P. Kolenko, P.J. Duskova, A. Stepankova, J. Hasek, J. Mol. Biol. 385 (2009) 1165, and references therein.
[97] M. Faraggi, I. Pecht, Nat. New Biol. 233 (1971) 116.
[98] A. Guissani, Y. Henry, L. Gilles, Biophys. Chem. 15 (1982) 177.
[99] P. O'Neill, E.M. Fielden, L. Morpurgo, E. Agostinelli, Biochem. J. 222 (1984) 71.
[100] O. Farver, I. Pecht, Mol. Cryst. Liq. Cryst. 194 (1991) 215.
[101] M. Machczynski, E. Vijgenboom, B. Samyn, G.W. Canters, Protein Sci. 13 (2004) 2388.
[102] O. Farver, A.W.J.W. Tepper, S. Wherland, G.W. Canters, I. Pecht, J. Am. Chem. Soc. 131 (2009) 18226.
[103] (a) K.A. Magnus, B. Hazes, H. Ton-That, C. Bonaventura, J. Bonaventura, W.G.J. Hol, Proteins 281 (1994) 302;
(b) T. Klabunde, C. Eicken, J.C. Sacchettini, B. Krebs, Nat. Struct. Biol. 5 (1998) 1084;
(c) M. Yasuyuki, T. Kumagai, A. Yamamoto, H. Yoshitsu, M. Sugiyama, J. Biol. Chem. 281 (2006) 8981.
[104] A.W.J.W. Tepper, L. Bubacco, G.W. Canters, J. Biol. Chem. 279 (2004) 13425.
[105] M. van Gastel, L. Bubacco, J.J. Groenen, E. Vijgenboom, G.W. Canters, FEBS Lett. 274 (2000) 228.
[106] H.-T. Li, T. Chang, W.-C. Chang, C.-J. Chen, M.-Y. Liu, L.-L. Gui, J.-P. Zhang, X.-M. An, W.-R.I. Chang, Biochim. Biophys. Res. Commun. 338 (2005) 1935.
[107] (a) O. Farver, P.M.H. Kroneck, W.G. Zumft, I. Pecht, Proc. Natl. Acad. Sci. U.S.A. 100 (2003) 7622;
(b) O. Farver, M. Brunori, F. Cutruzzolà, S. Rinaldo, S. Wherland, I. Pecht, Biophys. J. 96 (2009) 2849.
[108] I. Pecht, O. Farver, M. Goldberg, Adv. Chem. Ser. 162 (1977) 179.
[109] (a) R. Brändén, J. Deinum, FEBS Lett. 73 (1977) 144;
(b) R. Brändén, J. Deinum, M. Coleman, FEBS Lett. 89 (1978) 180.
[110] U.M. Sundaram, H.H. Zhang, B. Hedman, K.O. Hodgson, E.I. Solomon, J. Am. Chem. Soc. 119 (1997) 12525.
[111] J. Henry, J. Peisach, J. Biol. Chem. 253 (1978) 7751.
[112] F.J. Enguita, D. Marcal, L.O. Martins, R. Grenha, A.O. Henriques, P.F. Lindley, M.A. Carrondo, J. Biol. Chem. 279 (2004) 23472.
[113] E.I. Solomon, P. Chen, M. Metz, S.-K. Lee, A.E. Palmer, Angew. Chem. Int. Ed. 40 (2001) 4570.
[114] M. Goldberg, S. Vuk-Pavlovic, I. Pecht, Biochemistry 19 (1980) 5181.
[115] I. Bento, M.A. Carrondo, P.F. Lindley, J. Biol. Inorg. Chem. 11 (2006) 539.
[116] A.W.J.W. Tepper, S. Milikysiants, S. Scottini, E. Vijgenboom, E.J.J. Groenen, G.W. Canters, J. Am. Chem. Soc. 131 (2009) 11680.